NTNU – Trondheim
Norwegian University of
Science and Technology

# Heparin Analogs Created by Sulfation of Alginates Using a Chemoenzymatic Strategy

Øystein Arlov

Biotechnology (5 year)

Supervisor: Gudmund Skjåk-Bræk, IBT

Norwegian University of Science and Technology
Department of Biotechnology

# Preface

The work described in this thesis was carried out at the Norwegian Biopolymer laboratory (NOBIPOL), Department of biotechnology, in cooperation with the Department of cancer research and molecular medicine, at the Norwegian university of science and technology.

First and foremost I would like to thank my main supervisors Professor Gudmund Skjåk-Bræk and Dr. Finn Aachmann for the coordination of the project, invaluable advice and for the opportunity to participate in their inspiring work. I am very grateful to Professor Anders Sundan for supervision and coordination of the work carried out at the Department of cancer research and molecular medicine, and especially to Dr. Kristine Misund and Senior Engineer Hanne Hella for much needed aid and advice. I would also like to extend my thanks to Staff Engineers Wenche Iren Strand and Ann-Sissel Teialeret Ulset for their guidance with the laboratory work, and to Ph.D. Saepurahman Saepurahman at the Department of Chemistry and Dr. Minli Xie for their kind assistance with the infrared spectroscopy.

Lastly, I would like to thank Maren for her love and encouragement, as well as friends and family for their support.

NTNU, Trondheim
May 15th 2012

Øystein Arlov

# Abstract

Alginates are a class of natural unbranched linear polysaccharides, and consist of the monomers β-D-mannuronic acid and α-L-guluronic acid. The inherent physical properties, relative ease of modification, wide availability and good biocompatibility of alginates have gained a great deal of attention with regards to therapeutic applications. Heparin is a highly negatively charged linear glycosaminoglycan that is widely used as an anticoagulant. The presence of carboxyl groups and several sulfate groups gives heparin its negative charge, while iduronic acid moieties confer a high degree of flexibility to the polysaccharide by being able to assume different stable conformations. Heparin shows diversity in molecular weight, monomer sequence and modification pattern, resulting in a vast range of biological effects. When administered therapeutically, this can in cause an unpredictable dose response and potentially severe adverse effects in certain patients. The main objective of this study was to create a structural analog of heparin exhibiting a more regular structure and distribution, through chemical sulfation of alginate using chlorosulfonic acid. Other important aims were to characterize the analog in terms of structure, distribution and sulfation degree, and assess protein binding and anticoagulating properties of the sulfated alginates in comparison with heparin and the unmodified alginate templates.

Sulfation was performed using chlorosulfonic acid in formamide on a polymannuronic acid (poly-M) and a polyalternating alginate with a guluronic acid fraction of $F_G = 0.46$ (poly-MG), introduced through enzymatic epimerization. FTIR, elemental analysis with HR-ICP-MS and carbon NMR were employed to detect the attached sulfate groups on the alginate. The average molecular weights and the mass distributions of the alginate samples were studied using SEC-MALLS. Elemental analysis was used to estimate the sulfation degrees of the alginates, and $^{13}C$ NMR was employed to study substitution patterns, provide additional DS estimates and assess sample purity. The protein binding properties of the sulfated alginates were evaluated by studying their ability to release hepatocyte growth factor and osteoprotegerin bound to myeloma cells. Anticoagulating properties were studied by measuring prolongation of plasma coagulation time as a result of sulfated alginate supplementation.

The alginates were successfully sulfated and exhibited different degrees of sulfation obtained by varying the chlorosulfonic acid concentration used (1 - 10 %), as estimated by elemental analysis. The poly-MG alginate showed increased solubility during the sulfation reaction, resulting in a higher estimated DS at lower chlorosulfonic acid concentrations compared with poly-M. No apparent degradation of the alginates as a result of the sulfation was observed, although preliminary acid hydrolysis resulted in a molecular weight disparity between poly-M and poly-MG samples. Analysis of carbon NMR spectra allowed characterization of novel peaks and secondary DS estimations for the sulfated poly-M samples, while the complexity of the sulfated poly-MG spectra prevented confident characterization of the structures. Sulfation resulted in a profound improvement of the protein binding properties of the alginates, and showed prolongation of the plasma coagulation time at high treatment concentrations.

# Abstract - Norwegian

Alginater er en gruppe uforgrenede, lineære polysakkarider bygd opp av monomerene β-D-mannuronsyre og α-L-guluronsyre. De iboende fysiske egenskapene, modifikasjonsmulighetene, store tilgjengeligheten og den høye biokompatibiliteten til alginater har tiltrukket stor oppmerksomhet med henhold til terapeutiske applikasjoner. Heparin er et høyt negativt ladd molekyl i glykosaminoglykan-familien og er omfattende brukt som et antikoagulerende legemiddel. Karboksylgrupper og flere sulfatgrupper på monomerene gir heparin dets negative ladning, mens iduronsyre-monomerer tilfører molekylkjeden fleksibilitet ved å kunne innta ulike stabile konformasjoner. Heparin innehar en høy diversitet med henhold til molekylvekt, monomersekvens og modifikasjonsmønster, som resulterer i et bredt spekter av biologiske effekter som kan videre medføre en uforutsigbar respons til en gitt dose, samt potensielt alvorlige bivirkninger. Hovedhensikten med dette prosjektet var å lage en strukturell analog til heparin med en mer regelmessig struktur, gjennom kjemisk sulfatering av alginat ved bruk av klorsulfonsyre. Andre viktige mål var å karakterisere analogen med henhold til struktur, distribusjon og sulfateringsgrad, samt undersøke proteinbindende og antikoagulerende egenskaper i de sulfaterte alginatene sammenlignet med heparin og umodifiserte alginater.

Sulfatering ble utført ved bruk av klorsulfonsyre i formamid på en polymannuronsyre (poly-M) og en polyalternerende alginat med en guluronsyrefraksjon på $F_G$ = 0.46 (poly-MG), introdusert gjennom enzymatisk epimerisering. FTIR, elementanalyse med HR-ICP-MS og karbon-NMR ble gjennomført for å detektere sulfatgruppene på alginatet. De gjennomsnittlige molekylvektene og massedistribusjonene til de ulike alginatprøvene ble undersøkt ved bruk av SEC-MALLS. Elementanalyse ble videre brukt til å estimere sulfateringsgraden (DS) til alginatene, og $^{13}$C-NMR ble brukt til å undersøke studere substitusjonsmønster, gi et sekundærestimat av DS og bestemme prøvenes renhet. Proteinbindende egenskaper i de sulfaterte alginatene ble undersøkt ved å studere deres evne til å binde og frigjøre hepatocytt-vekstfaktor og osteoprotegerin fra overflaten av myelomceller. Antikoagulerende egenskaper ble studert ved å måle forlengelse av koagulasjonstiden til blodplasma som resultat av tilsatte sulfaterte alginater.

Alginatene ble sulfatert og viste ulike grader av sulfatering som resultat av varierende konsentrasjon av klorsulfonsyre brukt (1 - 10 %), estimert gjennom elementanalyse. Poly-MG alginatene viste høyere løselighet under sulfateringsreaksjonen, som resulterte i en høyere estimert DS ved lavere konsentrasjon av klorsulfonsyre, sammenlignet med poly-M. Det ble ikke observert noen betydelig degradering av alginatene som resultat av sulfateringen, men syrehydrolyse av alginatene i forkant av sulfateringen resulterte i ulik gjennomsnittlig molekylvekt for poly-M- og poly-MG-alginatene. Analyse av $^{13}$C-NMR spektre resulterte i en karakterisering av nye signaler oppstått fra sulfatering, samt en DS-estimasjon for de sulfaterte poly-M-alginatene, mens kompleksiteten i poly-MG-spektrene hindret tilsvarende karakterisering av alginatstrukturene med sikkerhet. Sulfatering av alginatene resulterte i en markant økning i proteinbinding, og viste ved høye konsentrasjoner en målbar forlengelse av koagulasjonstiden.

# Symbols and Abbreviations

| | |
|---|---|
| AT | Antithrombin III |
| dn/dc | Refractive index |
| DP | Degree of polymerization |
| DS | Degree of sulfation |
| $F_G$ | Guluronic acid monad fraction |
| FTIR | Fourier transform infrared spectroscopy |
| G | α-L-guluronic acid |
| GAG | Glycosaminoglycan |
| GlcA | β-D-glucuronic acid |
| GlcN | β-D-glucosamine |
| HCII | Heparin cofactor II |
| HGF | Hepatocyte growth factor |
| HIT | Heparin-induced thrombocytopenia |
| HR-ICP-MS | High resolution inductively coupled plasma mass spectroscopy |
| HS | Heparan sulfate |
| IdoA | α-L-iduronic acid |
| LMWH | Low-molecular weight heparin |
| M | β-D-mannuronic acid |
| MFI | Mean fluorescence intensity |
| $M_n$ | Molecular number average |
| $M_w$ | Molecular weight average |
| NAG | N-acetylglucosamine |
| NHP | Normal human plasma |
| NMR | Nuclear magnetic resonance |
| OPG | Osteoprotegerin |
| RPMI | Roswell park memorial institute (myeloma cell line) |
| SEC-MALLS | Size exclusion chromatography - multi-angle laser light scattering |
| S-M | Sulfated polymannuronic acid |
| S-MG | Sulfated polyalternating alginate of MG-blocks |
| UFH | Unfractionated heparin |

# Table of Contents

# 1 Introduction

## 1.1 Background

Heparin has been widely used as an anticoagulant since the discovery of its antithrombotic properties, and is used today primarily during surgery and as a prophylactic to treat a number of cardiovascular disorders. Although often fractionated and chemically modified, commercial heparin is still of mammalian origin, as the complexity and diversity of the molecule limits synthetic production to short oligomers (Bhaskar, Sterner et al. 2012). The inherent heterogeneity is correlated to the many observed physiological effects of heparin, complicating therapeutic use to effectively treat individual disorders while minimizing adverse effect. Finding alternative anticoagulating drugs with more limited number of interaction targets could reduce the incidences of excessive bleeding and immune reactions, and possibly bypass cases of heparin resistance. There have also been incidences with contamination of heparin batches (Li, Suwan et al. 2009), and the porcine origin of most commercial heparin also raises an issue when treating devout Muslim or Jewish patients. Although the heparin undergoes extensive chemical treatment during purification and is administered in relatively small amounts through injection rather than consumption, some Muslims and Jews still consider the drug forbidden unless used in life-threatening situations, where heparin is seldom used.

Alginate is a good candidate for creating a functional analog to heparin primarily due to its wide availability, good biocompatibility, structural similarity and several modification possibilities. Alginate is abundant in seaweeds and can be produced by bacteria in reactors. The relative ease of modifying the alginate structure enables creation of more specific polymeric drugs while retaining the biocompatibility of a natural compound. Genetically modified bacterial cultures can produce a pure polymannuronic acid template, allowing tailoring of the polymer using C5 epimerase enzymes in order to obtain specific sequence patterns. Structural similarity to heparin and an equally high charge density can be attained, as alginate monomers each have an inherent carboxyl group and two free hydroxyl groups susceptible to sulfation. Extensive research has elucidated new structure-function relationships in heparin, enabling the construction of analogous modification

patterns from an alginate template. An important difference between heparin and an alginate-based analog is that the latter can be modified to have a regularity in size, sequence and potentially sulfation pattern not seen in heparin. This is assumed to provide a more predictable drug response, and the sulfated alginates may have a more narrow range of physiological effects compared to the structurally disperse heparin.

## 1.2 Alginate

### 1.2.1 Structure and Physical Properties

Alginates are a group of unbranched polysaccharides primarily found in brown seaweeds, but is also produced by certain bacterial species, such as *Pseudomonas aeruginosa* and *Azotobacter vinelandii*. Bacterial alginates are commonly secreted extracellularly and used in biofilm formation or cyst generation (Rehm and Valla 1997), while in seaweeds the alginate serves as a structural component. Alginates are linear co-polymers consisting of the monomers β-D-mannuronic acid (M) and α-L-guluronic acid (G) (Figure 1). Naturally occurring alginates do not have regular repeating units, and the M- and G-units are either alternating or arranged in homopolymeric blocks of various lengths. Monomer distribution and block lengths are important characteristics of alginates as they have a significant impact on the physical properties.

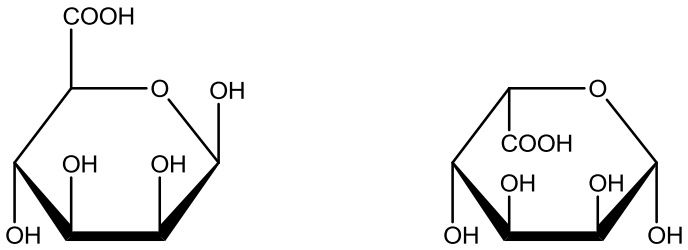


β-D-Mannuronic acid α-L-Guluronic acid

**Figure 1: Constituent monomers of alginate.**

The conformational difference between the monomers results in either diequatorial (M-M), equatorial-axial (M-G, G-M) or diaxial (G-G) bonding (Figure 2), leading to varying degrees of rotation and thus flexibility along the alginate chain. The diaxial bonds between adjacent G-monomers form cavities in the molecular structure of the alginate, allowing cooperative binding of divalent cations (e.g. $Ca^{2+}$, $Ba^{2+}$ and $Sr^{2+}$). The ions serve as cross-linkers and bind other alginate chains, ultimately forming a hydrated gel network (Smidsrød and Skjåk-Bræk 1990).

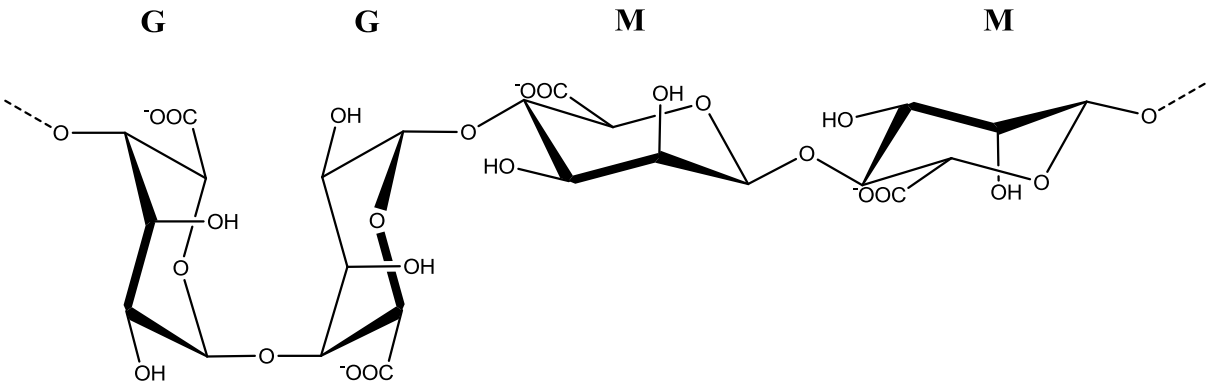


**Figure 2: Polymeric structure of alginate showing glycosidic bond orientations between monomers β-D-mannuronic acid (M) and α-L-guluronic acid (G)**

Alginates are polyelectrolytes, and are the only natural occurring polymers containing a carboxyl group on each constituent monomer (Ikeda, Takemura et al. 2000). The pK value of alginate is approximately 3.6 (Simsek-Ege, Bond et al. 2003), meaning that the carboxyl group is deprotonated at neutral pH, giving alginates an evenly distributed net negative charge. The flexibility of the alginate chains increases in the order GG<MM<MG (Smidsrød and Skjåk-Bræk 1990), as the axial-equatorial bonding confers less steric hindrance and thus an increased range of rotation compared to diequatorial linkage between two M monomers (Smidsrød 1973).

Molecular weight of alginates is an important factor in gel formation, affecting properties such as mechanical strength, porosity and swelling. It is also relevant for the application of alginate chains in solution, as high molecular weight alginates can significantly increase the viscosity of concentrated solutions. In a solution containing live cells, an increase in viscosity leads to higher mixing requirements to maintain sufficient mass

transport of gases and nutrients (Doran 1995). Shear forces from the mixing or injection of such viscous solutions may compromise proteins and cells present, which is highly relevant for the application of dissolved alginate in biological systems (Kong, Smith et al. 2003).

### 1.2.2 C5 Epimerization

Epimerization is a process whereby a diastereomer of a molecule is formed through re-configuration of a single stereogenic center. In nature epimerization of carbohydrates is catalyzed by enzymes known as epimerases and, in the case of polysaccharides, usually occurs prior to polymerization. However, certain epimerases can convert monomers post-polymerization without compromising the polymer backbone. Examples of such reactions are C5 epimerizations of D-mannuronic acid into L-guluronic acid in alginates, and D-glucuronic acid into L-iduronic acid during heparin and heparan sulfate (HS) synthesis (Valla, Li et al. 2001). During the epimerization process in alginates, carbon 5 of D-mannuronic acid is re-configured, forming the epimer L-guluronic acid. The most stable conformation for the M units is the $^4C_1$ chair, but during epimerization the hexapyranose ring will assume the inverted $^1C_4$ chair conformation. The switch alters the bond orientations and thus the overall conformation of the alginate chain, making epimerization a useful tool to alter the physical properties of alginate. Mutant bacterial strains can be utilized to produce pure polymannuronic acid (Gimmestad, Sletta et al. 2003), and different epimerases can be used to tailor the polymer, introducing specific sequence patterns *in vitro*.

In algae and bacteria, L-guluronic acid monomers of alginate are not synthesized *de novo*, but introduced through epimerization following chain assembly. Alginate-producing species are thus able to determine the physical properties of the polymer through controlled regulation and expression of various forms of the C5 epimerases. As alginate is an important structural component of the algae cell wall and intercellular spaces, as well as in bacterial biofilms and cysts, regulation of epimerization allows efficient adaptation to various environments. For instance, the commercially important seaweed *Laminaria hyperborea* has a relatively high content of G blocks in the stipe and outer cortex, while

the leaf has a lower content of G units that are primarily interspaced between M monomers (Smidsrød and Skjåk-Bræk 1990). The ability of continuous G blocks to bind $Ca^{2+}$ and form gels provides the mechanical strength and rigidity required to withstand environmental forces on the seaweeds.

Bacterial alginates are excreted and epimerized extracellularly, where they participate in the formation of protective layers such as viscous fluids or solid-like cysts. Alginate-producing bacteria have been shown to express a variety of calcium-dependent C5 epimerases and have been thoroughly studied for commercial application of the epimerases (Ertesvåg, Høidal et al. 1999), and additionally for their role in the progression of cystic fibrosis (Jain, Franklin et al. 2003). Alginate from studied species of the *Pseudomonas* genus does not exhibit G blocks and each G monomer is interspaced by at least one M (Skjåk-Bræk, Grasdalen et al. 1986). Epimerases from different *Azotobacter* species, however, introduce G and MG blocks in specific patterns. Of particular interest is the epimerase AlgE4, which exclusively introduces an alternating MG sequence along the alginate chain without G block formation (Ertesvåg, Høidal et al. 1999). Mannuronic acid monomers of bacteria-derived alginates have been found to exhibit various degrees of acetylation at the hydroxyl groups on carbons 2 and 3 (Skjåk-Bræk, Grasdalen et al. 1986). The lack of acetyl groups on guluronic acid monomers indicates that the added bulkiness on acetylated M units prevents epimerization by the enzymes, and that acetylation is an important factor for regulating alginate sequence in bacteria (Valla, Li et al. 2001).

### 1.2.3 Covalent Modification of Alginates

The alginate monomers are susceptible to a number of chemical modification reactions, enabling alteration of the polysaccharide's inherent properties, introduction of new properties and facilitation of additional intermolecular interactions. Together with the epimerization techniques utilized to manipulate monomer sequence, chemical modification of alginate can offer a vast variety of novel alginate derivatives.

Targeting the carboxyl group present on all alginate monomers, a common modification strategy employs carbodiimide molecules which can activate and expose the carboxylic group to a nucleophilic attack (Cathell, Szewczyk et al. 2010). As cells do not commonly attach to alginate due to its hydrophilic nature, previous work has been done to attach Arginine-Glycine-Aspartic Acid (RGD)-containing peptides to the carboxyl group of alginates to enable interaction and cell anchorage in immobilization and encapsulation systems. Here, the terminal amine nitrogen of the peptide functions as the nucleophile and forms an amide bond to alginate (Rowley, Madlambayan et al. 1999). The same strategy can be utilized to cross-link alginate with other sugars, as demonstrated by Donati and coworkers (2003) with the coupling of the carboxyl groups of the alginate monomers to the anomeric carbon of galactose via an amide bond (Donati, Vetere et al. 2003).

Alginate can be extensively modified at the free hydroxyl groups on C2 and C3, primarily through addition of small chemical groups or cross-linking reactions via ether or ester bonds. For instance, esterification with propyleneoxide forms propylene glycol alginate (PGA), a widely used derivative in the food industry (Draget, Skjåk-Bræk et al. 1997). Esterification to longer alkyl chains can lower the water solubility of alginate and promote hydrophobic interactions (Rastello De Boisseson, Leonard et al. 2004). Sulfate groups can be added to the available hydroxyl groups in order to improve blood compatibility and promote anticoagulating properties, similarly to heparin and heparan sulfate (HS). Sulfated alginates can easily be attained through reacting dried alginate with chlorosulfonic acid ($ClSO_3H$) in formamide (Huang, Du et al. 2003). Using an alternative strategy, sodium alginate is converted to a tertiary amine salt followed by sulfation using carbodiimide and sulfuric acid ($H_2SO_4$) (Freeman, Kedem et al. 2008). Both reactions are performed under strong acidic conditions, which can cause precipitation of the alginate and some degree of depolymerization in high molecular weight chains. A more recent

strategy involves synthesizing a sulfating agent without the use of strong acids, and has been successfully employed to sulfate alginate, chitosan and pectin (Fan, Jiang et al. 2011), (Fan, Wu et al. 2012), (Fan, Gao et al. 2012). The sulfating agent ($N(SO_3Na)_3$) was prepared from sodium bisulfate and sodium nitrate in an aqueous medium and allowed sulfation without any measureable degradation of the polysaccharides.

It is also possible to modify the hexose backbone of the alginate through a partial oxidation reaction using periodate, resulting in ring opening between C2 and C3 (Scott and Harbinson 1969). Periodate oxidation of 5 % of the uronic acid monomers retains most desired properties of the alginate such as gelling (Gomez, Rinaudo et al. 2007), while conferring increased flexibility and solubility, and decreased viscosity in solution. In contrast to non-oxidized alginate, the open-chain derivative is also susceptible to backbone degradation in an aqueous media under physiological conditions (Bouhadir, Lee et al. 2001).

The range and extent of possible modifications have been limited by a lack of solubility of alginates in organic solvents. Certain modification reactions in aqueous solutions also have clear disadvantages due to the low stability of alginate in very acidic, basic or reductive environments (Pawar and Edgar 2012). Complete organic solubility has, however, been achieved using a tetrabutylammonium (TBA) salt of alginic acid in a polar aprotic solvent of tetrabutylammonium fluoride (TBAF) with dimethyl sulfoxide (DMSO) (Pawar and Edgar 2011). Another challenge is achieving selectivity when modifying the hydroxyl groups of alginate. Due to the similar chemical environments of C2 and C3, most reactions affect both targets at equal frequencies (Pawar and Edgar 2012). However, conformational variations arising from different bond orientations between the M and G monomers may impose steric hindrance towards addition of bulky groups, causing favoring of one hydroxyl group over the other.

### 1.2.4 Therapeutic Use of Alginates

The gel-forming ability, biocompatibility, physical properties and vast modification possibilities make alginates suitable in a number of therapeutic applications. Gel-forming alginates have widespread use in hydrogel-based wound dressings and can function as carriers in drug delivery systems. Furthermore, chemically modified alginate derivatives can mimic the actions of physiologically important polysaccharides or assume new beneficial functions.

Hydrogel-based wound dressings are particularly useful in treating burn injuries. The most important desired properties of burn dressings are fluid absorption, in order to collect exudates and maintain a moist environment for effective reepithelialization and healing, and to serve as a barrier against microbial infections (Quinn, Courtney et al. 1985). Hydrogels are transparent, can absorb a large amount of fluid and can be shaped *in situ* to properly fit the wound. Additionally, substances such as antimicrobial drugs, cytokines and growth factors can be embedded in the gel matrix to prevent infection and aid regeneration of tissue (Balakrishnan, Mohanty et al. 2005). Alginate gels can also be used as an excipient in drug delivery systems due to their gentle gelling conditions that don't compromise the drug carried (Augst, Kong et al. 2006). Cells may also be encapsulated in alginate gel beads for use in bioreactors, and have also been proposed to function as a barrier against the immune system in foreign tissue transplants, while still allowing gas and nutrient exchange with the environment (Smidsrød and Skjåk-Bræk 1990).

Sulfated alginates have been shown in the laboratory to exhibit potent blood regulating properties, having structural and functional similarities to the anticoagulating glycosaminoglycan heparin. The structural flexibility of alginates can be increased through targeted epimerization, while sulfate groups provide additional negative charges to the anionic alginate, allowing charge-dependent binding to a number of physiologically important proteins. Sulfated alginates have previously been shown to increase blood clotting time (Huang, Du et al. 2003), (Fan, Jiang et al. 2011), probably due to direct or indirect interaction with factors in the coagulation cascade. Sulfated alginates can also bind growth factors such as fibroblast growth factors (FGF) (Freeman, Kedem et al. 2008), and can thus affect angiogenesis when administered intravenously. In a different study, Hu and colleagues (2004) observed antitumor activity when administering

oligosaccharide derivatives of sulfated alginates to mice. While no direct cytotoxic effects were seen, the oligomers were suggested to have an indirect effect through stimulation of the host-mediated immune system, and could potentially be applied as an adjuvant in cancer therapy (Hu, Jiang et al. 2004).

Alginate as a food additive is generally recognized as safe (GRAS) by the Food and Drug Administration (FDA). It has been widely used as an additive due to its ability to hold water, form thermally stable gels and stabilize phases in a number of food products (Glicksman 1987). Alginate itself is not toxic to cells and has negligible immunogenicity, but can carry contaminants from the source organism or from the extraction process. Highly immunogenic lipopolysaccharide (LPS) may be associated with the alginate from bacterial isolates (Breger, Lyle et al. 2009), while seaweed extracts contain traces of toxic polyphenols and require purification (Smidsrød and Skjåk-Bræk 1990). Regardless of purity, alginate gel implants used for drug- or cell encapsulation may still be recognized as foreign bodies, resulting in an inflammatory response with fibrous capsule formation around the implants and impediment of the mass transport (Klock, Pfeffermann et al. 1997).

Implanted alginate gels dissolve following sequestration of the cross-linking cations, while complete clearance of free alginate chains from the circulation requires renal excretion. Chains with a molecular weight under 48 kDa/mol are readily excreted into the urine, while the larger fraction remains in the circulation (Alshamkhani and Duncan 1995). Mammals are unable to degrade the alginates due to a lack of the enzyme alginase. However, partial oxidation through periodate treatment renders the alginate susceptible to hydrolysis in a physiological environment, allowing degradation into lower-weight chains (Lee and Mooney 2012).

## 1.3 Heparin

### 1.3.1 Heparin Structure and Distribution

Heparin is a linear polysaccharide in the glycosaminoglycan (GAG) family. The relatively high density of sulfate groups makes it the most negatively charged biological polymer to be characterized (Jones, Beni et al. 2011). Heparan sulfate (HS) is a GAG similar to heparin in backbone structure, but is less sulfated and contains fewer α-L-iduronic acid (IdoA) residues (Yu and Chen 2007). While heparin is released as soluble chains through exocytosis, HS remains bound to the cell surface via a transmembrane linker protein. Heparin can be extracted from mast cells of various animal mucosa, but commercial-scale production is today primarily from porcine intestine (Bhaskar, Sterner et al. 2012). The two-dimensional structure of heparin consists of repeating disaccharides of β-D-glucosamine (GlcN) and an uronic acid, which may be β-D-glucuronic acid (GlcA) or α-L-iduronic acid (IdoA). The constituent monomers exhibit a varying substitution pattern, introduced during biosynthesis of heparin and HS. The ammonium group of the GlcN moiety may be N-sulfated, acetylated or unmodified ($NH_3^+$), and sulfate groups can be added to 3-O and 6-O positions in varying patterns. The uronic acids may be either unmodified or 2-O sulfated (Figure 3) (Jones, Beni et al. 2011).

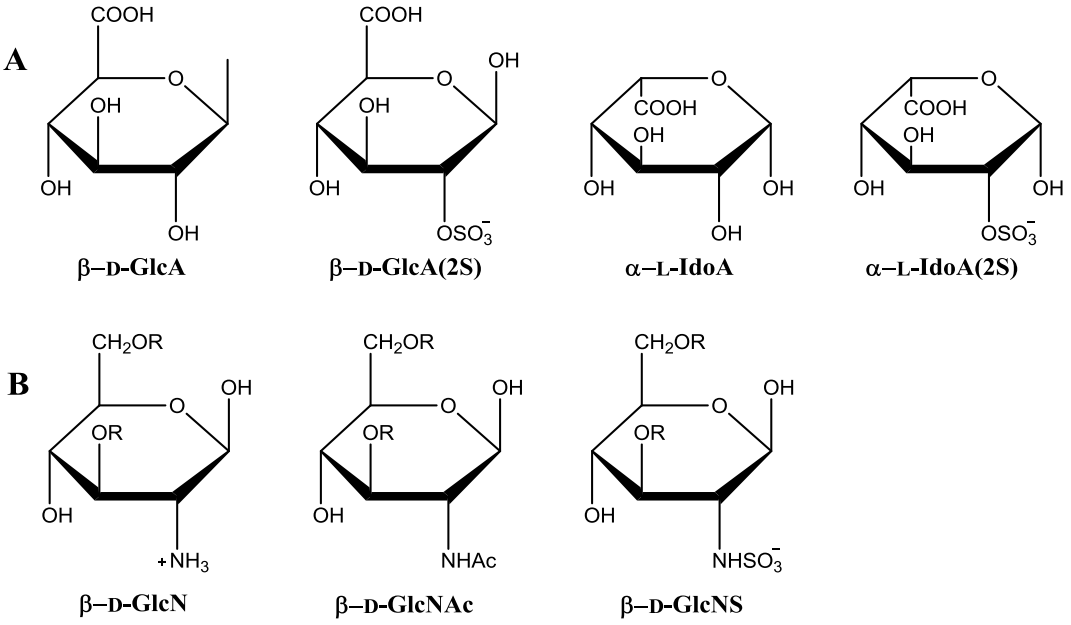


**Figure 3: Constituent monomers of heparin: (A) Uronic acids β-D-glucuronic acid (β-D-GlcA) and α-L-iduronic acid (α-L-IdoA), unsubstituted or with 2O-sulfation (2S). (B) Amino sugars β-D-glucosamine (β-D-GlcN), unsubstituted, N-acetylated or N-sulfated (R = H or $SO_3^-$).**

Therapeutic heparin can be divided into two main classes based on mean molecular weight: unfractioned heparin (UFH) and low-molecular weight heparin (LMWH). UFH has a weight distribution of 3 - 30 kDa/mol with a mean of 15 kDa (Hirsh, Anand et al. 2001), while the weight range of LMWH is 1 - 10 kDa with a mean between 4 and 5 kDa/mol (Hirsh 1998). Additionally, some recently derived drugs are based on an ultra low-molecular weight heparin (ULMWH) oligosaccharide, with high selectivity for specific interactions in the coagulation cascade (Bhaskar, Sterner et al. 2012), (Petitou and van Boeckel 2004).

### 1.3.2 Physical Properties of Heparin

The L-iduronic acid component of heparin gives heparin its high inherent flexibility, as the ring can assume three different conformations: chairs $^{1}C_{4}$ and $^{4}C_{1}$, and the skew-boat $^{2}S_{0}$ (Figure 4) (Sasisekharan and Venkataraman 2000). While the $^{2}S_{0}$ has been shown to be the active conformation in important interactions such as antithrombin III (AT) binding, it is likely that the molecular environment (e.g. neighboring monomers and interaction targets) as well as chemical factors such as salt concentration and pH can affect the current conformation of IdoA (Petitou and van Boeckel 2004), (Ernst, Venkataraman et al. 1998). This flexibility, in addition to the sequential heterogeneity of the polysaccharide, is assumed to contribute to the observed versatility of heparin in regulatory interactions (Rees, Morris et al. 1985).

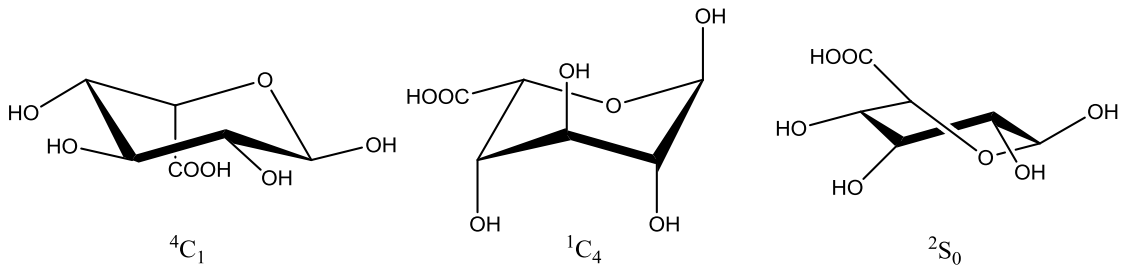


**Figure 4: Structural conformations of α-L-iduronic acid in heparin and heparan sulfate.**

### 1.3.3 Biosynthesis and Post-Glycosylational Modification

Heparan sulfate (HS) is expressed in all types of cells as a constituent of the extracellular matrix, while heparin is synthesized exclusively in mast cells (Parra, Veraldi et al. 2012). Both GAGs are produced and modified in the Golgi apparatus. Starting chains of four monosaccharides each are attached to a core protein and disaccharides of GlcA and N-acetylglucosamine (NAG) are subsequently added to the growing chains by glycosyltransferase enzymes (Sasisekharan and Venkataraman 2000). As with the alginate presented above, the synthesis of heparin and HS is not template driven, resulting in chains of highly variant lengths, consisting of 10-200 disaccharide units (Orgueira, Bartolozzi et al. 2003). The nascent chains of alternating GlcA and NAG are then modified in a series of reactions, resulting in biologically active heparin and heparan sulfate. For heparin, the peptide core of the proteoglycan intermediate is cleaved and the polysaccharide is endocytosed into secretory granules within the mast cells (Conrad 1998).

The enzymatic modifications occur either concurrently or in a sequence of independent steps (Sasisekharan and Venkataraman 2000). Most of the NAG monomers added during synthesis are deacetylated, forming a substrate for N-sulfation. Furthermore, N-sulfation is a prerequisite for subsequent C5 epimerization of D-glucuronic acid into L-iduronic acid, as well as O-sulfation (Jacobsson, Riesenfeld et al. 1985). The major sites for O-sulfation are C6 on the amino sugar residues (GlcNAc and $GlcNSO_3H$) and C2 on IdoA. Less frequent sulfation occurs at C3 of $GlcNSO_3H$ and at C2 of the non-epimerized GlcA moieties (Kusche and Lindahl 1990). Enzymes involved in the biosynthesis and modification of GAGs are known to have several tissue-specific isotypes, as shown for sulfotransferases by Habuchi and coworkers (Habuchi 2000). Different isoforms commonly have unique substrate specificities and most modification reactions are incomplete, resulting in varying patterns and extents of heparin modifications (Jacobsson, Riesenfeld et al. 1985).

### 1.3.4 Anticoagulating Action and other Functions

Although heparin is used mainly as an anticoagulant to treat various cardiovascular disorders, the complexity and disparity of the molecule implicates it in other known, and probably several unknown, biological interactions.

During the coagulation cascade, the extrinsic and intrinsic pathways coalesce in a common pathway with the conversion of factor X to its active form, Xa. Factor Xa cleaves prothrombin, forming the active serine protease thrombin which ultimately produces and stabilizes the insoluble fibrin clot (Triplett 2000). Heparin binds the plasma cofactor antithrombin III (AT) through a specific pentasaccharide sequence (Figure 5) forming a complex and accelerating the action of AT as a coagulation factor inhibitor.

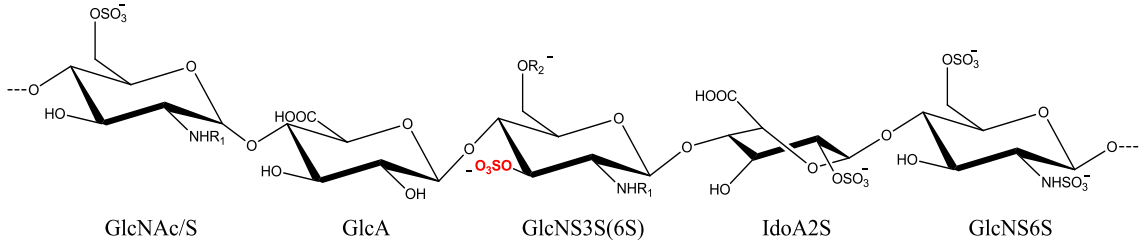


**Figure 5: The antithrombin III-binding pentasaccharide sequence in heparin ($R_1$ = acetyl or $SO_3^-$, $R_2$ = $SO_3^-$ or H). The outlined sulfate group on GlcNS3S(6S) is considered essential to AT binding. Adapted from (Chen and Liu 2005).**

While thrombin and factor Xa are the most sensitive targets (Hirsh and Raschke 2004), the heparin/AT-complex is also involved in the neutralization of several other factors such as factor IXa (Wiebe, Stafford et al. 2003) and tissue factor-bound VIIa (Lormeau, Herault et al. 1996). While associated with AT, heparin binds thrombin in a charge-dependent manner requiring at least 18 monosaccharides in the chain, increasing in effectiveness with chain length (Hirsh and Raschke 2004). On the other hand, Factor Xa inhibition appears to require only the pentasaccharide sequence in heparin associating with AT (Casu, Oreste et al. 1981), and is therefore the most prominent effect in low-molecular weight fractions of heparin.

Two additional anticoagulating effects of heparin are described, which function independently of AT and thus do not require the specific pentasaccharide sequence. The first involves non-specific binding and complex formation of heparin with heparin cofactor II (HCII), followed by thrombin inhibition by the complex. Although the activation mechanisms of HCII are similar to those for AT, the interaction is non-specific and depends on the charge and molecular weight of heparin. In contrast to AT, active HCII is capable of inhibiting fibrin-bound thrombin by using an alternative binding site (Huntington and Baglin 2003). HCII activation by heparin has been demonstrated with a minimal chain length of 13 monosaccharides, and the resulting thrombin inactivation is increased 2000-fold when doubling the heparin molecular weight (Okeeffe, Baglin et al. 2004). However, the lacking specificity of the heparin-HCII interaction results in a binding affinity approximately 1000 times lower than that for heparin and AT (Huntington and Baglin 2003). The second AT-independent anticoagulating function of heparin involves charge-dependent binding to factor IXa, which in turn blocks factor Xa generation (Weitz, Young et al. 1999). Similarly to HCII binding, the interaction lacks specificity and high concentrations of heparin are required to achieve an appreciable therapeutic effect (Hirsh and Raschke 2004).

Heparin also affects coagulation through platelet interactions. An indirect anticoagulating effect is inhibition of thrombin by the AT/heparin complex, thus reducing thrombin-induced platelet aggregation (De Candia, De Cristofaro et al. 1999). Heparin can also bind platelets directly through integrins on the platelet surface. High-molecular weight heparin chains appear to accommodate sufficient binding sites for both AT and platelets, while for low-molecular weight heparin, subfractions with low affinity for AT predominate in platelet binding (Salzman, Rosenberg et al. 1980). Although the response may vary depending on experimental conditions and the presence of interfering factors, heparin binding to platelets generally induces increased platelet responsiveness and activation (Gao, Boylan et al. 2011), despite the inhibition of thrombin-induced platelet activation mentioned above. Platelet aggregation may complicate the heparin treatment by opposing the anticoagulating effects and possibly contributing to non-beneficial thrombosis.

Heparin and heparan sulfate have been shown to interact with and possibly influence the infectivity of certain animal viruses. Envelope proteins of dengue virus and herpes simplex virus bind highly sulfated motifs on cell surface HS chains, which is assumed to be a requirement for cell entry. Heparin can reversibly bind the same envelope proteins, inhibiting cell attachment of the viruses and reducing the infectivity of the viruses (Chen, Maguire et al. 1997), (Shukla, Liu et al. 1999), (Nahmias and Kibrick 1964).

Heparin and HS are assumed to have an active regulatory role in cell proliferation, through the binding and stabilization of growth factors such as fibroblast growth factor 2 (FGF-2) (Forsten, Fannon et al. 2000). Heparin also binds to the cytokine hepatocyte growth factor (HGF) with high affinity, and can release the protein bound to heparan sulfate on the cell surface and extracellular matrix (Seidel, Hjorth-Hansen et al. 1999), as well as from the HGF receptor c-met expressed on myeloma cells (Børset, Hjorth Hansen et al. 1996).

Several factors in the clotting and fibrinolytic pathways, including aforementioned antithrombin III, have been proposed to also have important roles in angiogenesis (O'Reilly, Pirie-Shepherd et al. 1999). The direct and indirect interactions of heparin with these factors are thus likely to affect the formation of new blood vessels. In fact, low-molecular weight heparin fractions have been demonstrated to have an anti-proliferative effect on endothelial cells in a manner both dependent on chain length and specific monomer modifications (Khorana, Sahni et al. 2003). The apparent antiangiogenic effects and growth factor-modulating properties have led to a lot of research on low-molecular weight heparin as an adjuvant in cancer therapy, and have in several cases been suggested to counteract tumor growth and metastasis (Castelli, Porro et al. 2004), (Kragh, Binderup et al. 2005). However, a recent study showed that the overall survival rate in several common cancer types is not improved by LMWH treatment, and that the beneficial effects of heparin in cancer treatment thus remain controversial (van Doormaal, Di Nisio et al. 2011).

### 1.3.5 Heparin Limitations

Heparin fractions with a wide distribution regarding size, sequence and modification pattern can have an equally wide range of pharmacodynamic properties, potentially causing complications when treating individual disorders. As described below, there are also pharmacokinetic obstacles arising when treating a patient with heparin, where some of these limitations can be overcome by utilizing low-molecular weight fractions (LMWH).

Several of the pharmacokinetic limitations of unfractionated heparin as an optimal anticoagulant stem from charged-dependent non-specific binding to proteins and cell surfaces (Hirsh, Anand et al. 2001). Certain plasma components, as described with the abundant glycoprotein vitronectin (Preissner and Muller-Berghaus 1987), can bind and sequester heparin as well as low weight derivatives, resulting in reduced bioavailability. Molecular weight also affects the clearance rate of heparin from the circulation. Longer chains are cleared more rapidly, resulting in accumulation and prolonged action of low-weight chains primarily inhibiting factor Xa, with minor effects on thrombin (Hirsh and Raschke 2004). Additionally, binding to macrophage and endothelial cell surfaces can facilitate increased clearance of heparin (Hirsh, Anand et al. 2001). The shorter chain length of LMWHs causes less efficient protein- and cell surface binding, resulting in increased bioavailability following administration, as well as prolonged action (Hirsh 1998). The extent of these pharmacokinetic disadvantages may vary between individual patients, resulting in a less predictive response to a fixed dose of heparin. As previously mentioned, heparin complex formation with AT requires a specific pentasaccharide sequence which is present in approximately one third of isolated heparin molecules. Consequently, two thirds of the administered heparin do not bind AT and have low anticoagulating abilities, independent of weight fractioning (Lam, Silbert et al. 1976).

An important and relatively common condition is heparin resistance, where the patient shows reduced responsiveness to heparin and requires a significantly larger dose to obtain a therapeutic effect. The diminished response can be ascribed to several pharmacokinetic mechanisms affecting the bioavailability of heparin, but is in most clinical scenarios associated with an antithrombin III deficiency (Bar-Yosef, Cozart et al. 2007). AT

deficiency can be a genetic trait, but low AT levels are more commonly caused by prolonged exposure to intravenous heparin (Marciniak and Gockerman 1977). Heparin is widely used during surgery to counter anticoagulation triggered by endothelial damage. Patients undergoing cardiac surgery commonly receive heparin preoperatively, which can cause heparin resistance through AT depletion, limiting the action of heparin administered during surgery (Bar-Yosef, Cozart et al. 2007). The effect can in part be alleviated by supplementation of AT through fresh frozen plasma (Sabbagh, Chung et al. 1984) or by increasing the dose of heparin, although the latter alternative may lead to adverse complications such as increased bleeding. To avoid hypotension and bradycardia, cases of excessive bleeding are normally treated through intravenous injection of a neutralizing heparin antagonist, such as protamine (Hirsh and Raschke 2004).

Heparin has in some cases been shown to contribute to osteoporosis by binding and inhibiting the cytokine osteoprotegerin (OPG). OPG functions as an inhibitor of the NFκB ligand RANKL, which is secreted by osteoblasts to limit the activity of osteoclasts. Inhibition of OPG by heparin can thus result in osteoclast-induced bone resorption (Irie, Takami et al. 2007). The extent of osteoclast stimulation has been shown to be highly dependent on heparin size and sulfation pattern, where LMWH and N-desulfated heparin showed a reduced degree of bone resorption compared with the respective high-molecular weight and high-sulfate counterparts (Shaughnessy, Young et al. 1995). LMWH has been recommended for long-term use during pregnancy to decrease incidences of miscarriages (Greer and Hunt 2005). Although lactating women already have an increased calcium turnover from bone reserves, the heparin treatment is thought to have an additive impact on bone resorption, but the severity of the effect remains inconclusive (Lefkou, Khamashta et al. 2010).

Heparin-induced thrombocytopenia (HIT) is a severe adverse effect from heparin therapy with an estimated incidence of 1-5 % in treated patients (Kelton 2002). The complication is initiated by the release of a small platelet factor, PF4, from activated platelets. Some of the PF4 molecules remain associated with the platelet surface and facilitate charge-dependent binding to heparin in the circulation. The complex acts as an epitope and is recognized by IgG antibodies. Receptors on the platelet surface consequently bind to the Fc region of the antibodies, leading to aggregation and further activation of the platelets, thus reinforcing the effect (Franchini 2005). These events extensively activate the

coagulation cascade, which can ultimately lead to thrombosis and cardiovascular complications in patients. Thrombocytopenia refers to a platelet decrease in the circulation, which in this case is caused by increased clearance of activated IgG-bound platelets (Chong 2003). Similarly to the effects of heparin on bone resorption described above, treatment with low-molecular weight fractions resulted in a lower incidence of HIT, likely due to reduced PF4 and platelet binding (Warkentin, Levine et al. 1995), (Hirsh and Raschke 2004).

As commercial heparin is isolated from mammalian cells, contamination is possible and can cause additional adverse effects in the treated patients. The isolate can carry pathogens such as avian influenza virus or prions associated with bovine spongiform encephalopathy, depending on the source (Mendes, dos Santos et al. 2009). In 2008, several heparin batches as well as LMWH derivatives had to be withdrawn due to a contamination of chondroitin sulfate (CS), a glycosaminoglycan with a higher negative charge density than heparin. CS has relatively low anticoagulant activity, but can cause bradykinin production through the kinin-kallikrein pathway. Bradykinin causes vasodilation which can further lead to a severe drop in blood pressure (Li, Suwan et al. 2009).

## 1.4 Structural Characterization

### 1.4.1 SEC-MALLS

Similarly with many other natural polysaccharides the synthesis of alginates is not template based, resulting in a range of different sized chains. When describing alginate chain size, commonly used characteristics are the molecular weight average ($M_w$) and the average number of monomers composing each chain, known as degree of polymerization (DP).

Light scattering is an effective technique for determining the absolute mass of macromolecules, and can also give conformational data on polymers in solution. As the name implies, the principle of the technique is based on the fact that particles in a solution scatter light when irradiated. The incident light beam can be thought of as an oscillating electrical wave causing displacement of electrons, forming a dipole within the molecule. The dipole itself will in turn oscillate and emit new radiation in the form of scattered light. The amount of scattered light increases with the polarizability of the molecule, which is directly proportional to the refractive index (dn/dc) parameter characteristic for a polymer solution (Podzimek 2011). When studying small globular proteins with a narrow weight distribution, classical light scattering measured at a single angle is sufficient, as the intensity of the scattered light will be uniform in all directions. Size Exclusion Chromatography - Multi-Angle Laser Light Scattering (SEC-MALLS) is a technique more often employed when studying polysaccharides, which have a more extended conformation and can have a wide molecular weight distribution. Here, light scattering is measured at several angles, allowing mass determination of larger macromolecules as well as measurement of the geometric size of the individual molecules, expressed as the radius of gyration ($R_G$ or $R_Z$). Injection of the sample through a size-exclusion column prior to detection results in a mass distribution curve where larger molecules are eluted out first, allowing analysis of the weight range of the individual samples and the relative disparity between samples. For the purpose of analyzing sulfated alginates, the SEC-MALLS data can additionally be used to assess degradation of the sulfated samples compared to an unmodified reference sample.

The molecular size averages measured in light scattering are the molecular number average ($M_n$) and molecular weight average ($M_w$) shown in equations 1.1 and 1.2, respectively. $M_n$ is commonly expressed in terms of moles (n), where $M_i$ is the polymer molecular weight. The more frequently used $M_w$ emphasizes the impact of large chains, by incorporating the gathered mass of each polymer size in the sample, expressed as w.

$$M_n = \frac{\sum_{i=1}^{n} n_i M_i}{\sum_{i=1}^{n} n_i} \qquad (1.1)$$

$$M_w = \frac{\sum_{i=1}^{n} w_i M_i}{\sum_{i=1}^{n} w_i} \qquad (1.2)$$

The average number of monomers per alginate chain, or degree of polymerization (DP) is given by molecular number average divided by the monomer molecular weight ($M_0$), shown in equation 1.3. The polydispersity of the samples expresses the width of the weight distribution and is calculated by dividing the molecular weight average by the number average (equation 1.4). A polydispersity value of one corresponds to uniform chain length in the solution, and the value increases with the width of the weight distribution.

$$DP = \frac{M_n}{M_0} \qquad (1.3)$$

$$Polydispersity = \frac{M_w}{M_n} \qquad (1.4)$$

### 1.4.2 NMR Spectroscopy

Nuclear magnetic resonance (NMR) spectroscopy is the most widely used tool for structural characterization of organic molecules. The instruments and techniques have evolved profoundly over the last decades, allowing effective characterization of structure patterns, connectivity and dynamics in increasingly complex molecules. NMR spectroscopy is based on the presence of a nuclear spin momentum in certain atoms, therein most importantly $^{1}H$ and $^{13}C$. When a static magnetic field is applied to a molecule in solution, a magnetic dipole arises and the nuclei orient themselves either parallel or antiparallel to the magnetic field (Lehninger, Nelson et al. 2008). During an NMR experiment the sample is irradiated with an electromagnetic pulse, causing the nuclei of the molecule to resonate at a frequency characteristic of the atom, its connectivity and molecular environment. Many of the atoms in a molecule are in a unique electromagnetic environment primarily due to associated electrons that create localized small magnetic fields when moving. Nearby electrons have a partially shielding effect on the nucleus, which counters the applied magnetic field and decreases the resulting resonance frequency. Conversely, less electrons around the nucleus means that the nucleus is exposed to a stronger magnetic field, causing it to resonate at a higher frequency (Doucleff, Hatcher-Skeers et al. 2011). Thus, one molecule can give rise to several resonating sine waves at a number of different frequencies increasing with the complexity of the molecule. This collection of wave signals is expressed as amplitude as a function of time, and is translated into an NMR spectrum through Fourier Transformation (FT). This operation organizes the individual signals in a plot with amplitude as a function of frequency, where a peak is assigned to each unique frequency (Figure 6). The characteristic resonance patterns of atoms and knowledge of the electromagnetic influences within the molecule form the basis for obtaining structural data from an NMR experiment.

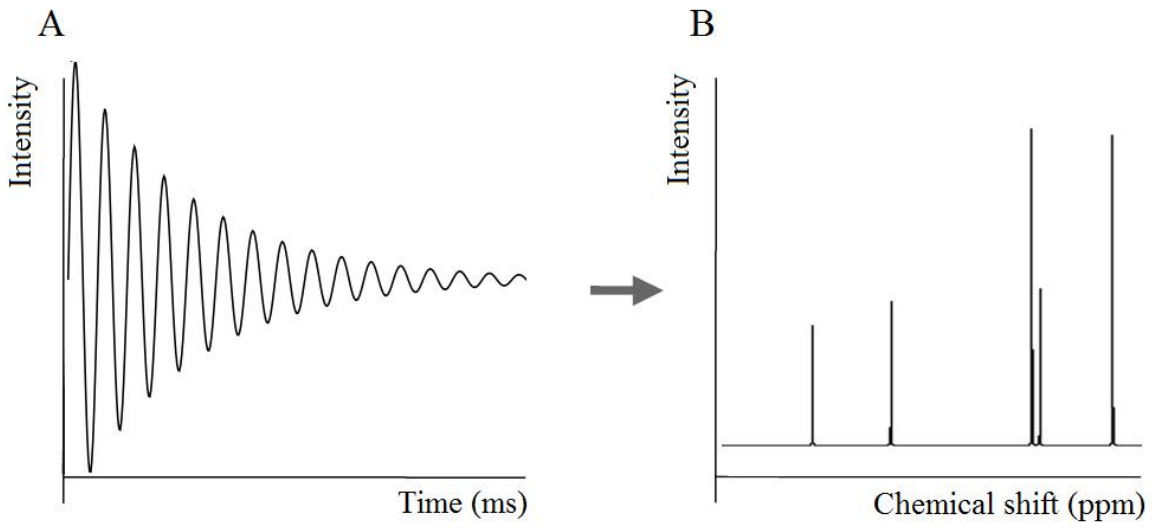


**Figure 6: Fourier transformation of NMR signals in a (A) time-domain spectrum into a (B) frequency-domain spectrum. Adapted from (Doucleff, Hatcher-Skeers et al. 2011)).**

Interpretation of the NMR spectrum becomes more challenging when studying complex macromolecules such as proteins or polysaccharides. Structural data of such molecules can be achieved through the employment of various multidimensional NMR techniques. The nuclear spins of atoms are coupled to one another in the sense that magnetization can be transferred between them. This energy transfer can occur across a covalent bond, also known as J-coupling, or can be obtained with spatially close atoms through the phenomenon called the nuclear Overhauser effect (NOE). Multidimensional spectra provide information about the connectivity and spatial arrangement of the atoms through the correlation of frequency signals, allowing deciphering of otherwise complex one-dimensional spectra.

Proton and carbon NMR spectroscopy is commonly employed to determine the relative content of M and G units in alginates as well as the overall monomer sequence. To obtain an optimal NMR spectrum from an alginate sample it is beneficial to hydrolyze the alginate chains to reduce sample viscosity, while a calcium chelator such as triethylenetetraamine (TTHA) may be added to samples with high guluronic acid content to prevent aggregation and partial gelling. Additionally, alginate samples dissolved in deuterium oxide are commonly run at a high temperature (90 $^{o}$C) to increase molecular motion and thus increase the resolution of the spectra (Grasdalen, Larsen et al. 1981). For the purpose of obtaining sequence data, it is convenient to divide the polymer sequence

into a collection of diads (MM, GG and MG) and triads (MMM, MMG, MGM, MGG, GMM, GMG and GGG). Electromagnetic coupling affects the resonance frequencies associated with an alginate monomer across the glycosidic bond, giving rise to distinguishable peaks depending on the identity of the adjacent monomers (Grasdalen, Larsen et al. 1981). Triad sequences can thus be assigned to these unique peaks, and the relative intensities can be used to calculate the triad fractions in the alginate sequence. The same principle can be applied when studying chemically modified alginates, as the addition of a new chemical group gives rise to novel chemical shifts in the spectrum. Interpretation of the spectrum becomes more challenging as the novel signals can be relatively weak and are also affected by neighboring monomers that can be either modified or unmodified. In the case of sulfation, each monomer can additionally have zero, one or two substitutions, further complicating the spectrum. Quantification of such chemical modifications to alginates thus requires high resolution spectra, sufficiently purified samples and unambiguous peak assignment.

### 1.4.3 Infrared Spectroscopy

Molecular covalent bonds are not static entities, and can undergo a number of vibrating motions. Analogous to a spring, a chemical bond can be stretched or bent in manners characteristic to the attached atoms and the electrostatic environment (Figure 7). Variations of these basic motions include symmetric and asymmetric stretching and in- and out-of-phase bending, also contributing to the IR spectrum (Stuart 2004).

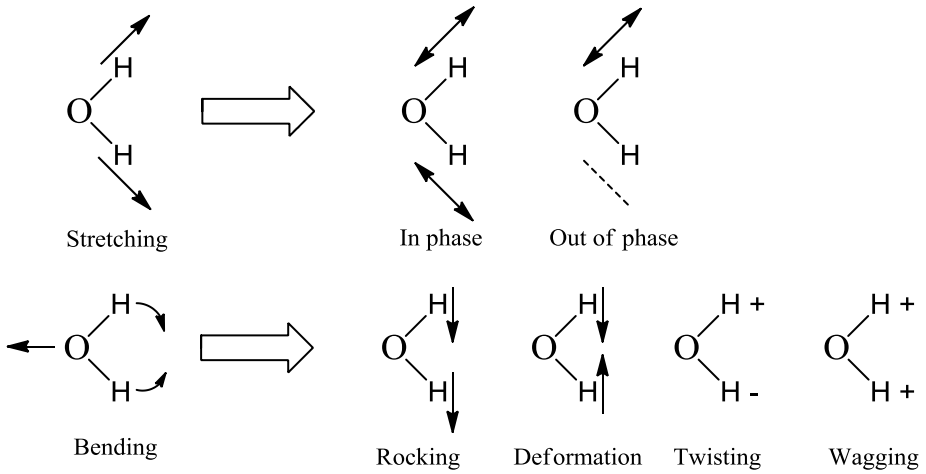


**Figure 7: Examples of basic motions of molecular bonds shown in a water molecule. Adapted from (Stuart 2004)).**

In normal modes of vibration all atoms in a molecule oscillate at the same frequency about their equilibrium position (Lambert 1998), but when a sample is irradiated with an electromagnetic beam, radiation in the infrared region is absorbed. Absorbed radiation is converted to molecular vibration, causing a transition between vibrational energy levels E1 and E2, where the energy difference between the two states is related to the frequency of the radiation (Lambert 1998). To obtain the IR spectrum, the recorded interference in transmission is transformed into either an absorption or a transmittance spectrum through Fourier transformation (FT) and plotted as a function of frequency, usually expressed in wavenumbers ($cm^{-1}$) (Figure 8). Different motions of each bond (e.g. stretching or bending) absorb radiation at different frequencies giving rise to unique absorption bands in the IR spectrum. As some of these peaks are prominent and characteristic of a certain bond, an IR spectrum can be used to obtain structural information about the molecule. IR can also be used to assess the purity of a sample, or to identify new chemical bonds in a molecule through comparison with reference spectra which are widely available.

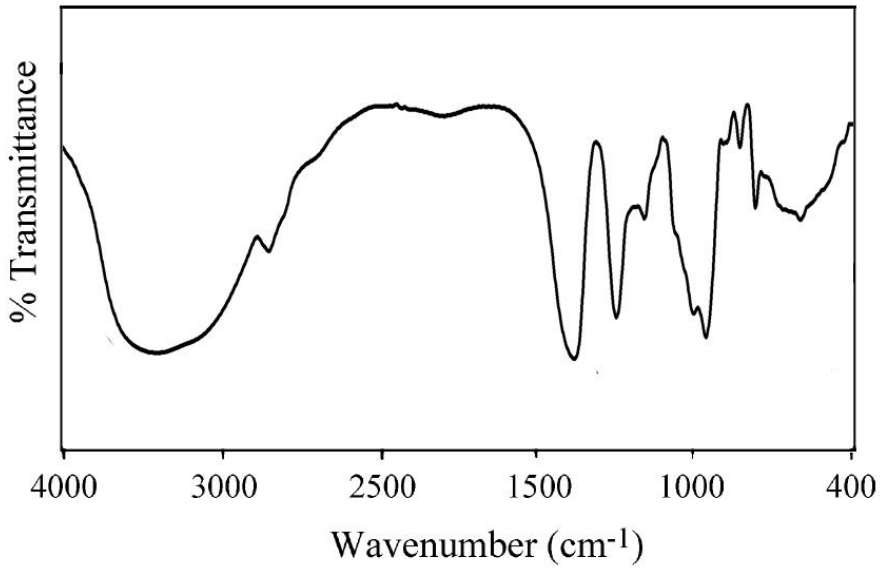


**Figure 8: FTIR transmission spectrum of sodium alginate. Adapted from (Zhu, Yang et al. 2007)**

For alginates, FTIR can be used to estimate the proportion of M to G units by measuring the relative intensities of bands characteristic for each monomer (Sakugawa, Ikeda et al. 2004). It is additionally a very useful technique to detect new chemical bonds from covalent modification reactions, as new peaks will appear when compared to an unmodified reference sample. It is, however, difficult to make precise quantitative assumptions from FTIR data as the absorption peak intensities are directly correlated to molecule concentration, necessitating meticulous sample preparation and instrument operation.

## 1.5 Aims of the Study

The main objectives of the study were to create a heparin analog based on a chemically sulfated alginate, characterize it and assess protein binding and anticoagulating properties.

Different concentrations (1-10 %) of the sulfating reagent were used to achieve different degrees of sulfation, while enzymatic epimerization was employed to increase the flexibility of the alginate. An important aim was to thoroughly characterize the structural properties of the sulfated alginates in terms of sequence, molecular weight, modification pattern and sulfation degrees in order to propose optimal properties for potential therapeutic use. To determine sulfation degrees, the modified alginates were studied using quantitative $^{13}$C-NMR techniques and through elemental analysis. NMR was also employed to study the modification pattern and assess selectivity of sulfation sites on the alginate when using the current modification techniques. Interaction between the sulfated alginate and known heparin-binding proteins was studied, and anticoagulating properties were investigated through a blood plasma clotting assay.

# 2 Materials and Methods

## 2.1 Materials

Epimerization and sulfation was performed on a purified polymannuronic acid ([η] = 940 ml/g) produced from an AlgG negative strain of *Pseudomonas fluorescens* (Gimmestad, Sletta et al. 2003), by NOBIPOL, Trondheim, Norway. AlgE4 enzyme was isolated from *Hansenula polymorpha*, by SINTEF Trondheim, Norway. 99 % chlorosulfonic acid ($ClSO_3H$) used for sulfation of alginates, as well as >= 99.5 % 4-Morpholinepropanesulfonic acid (MOPS) used in epimerization, was purchased from Sigma-Aldrich Norway AS (Oslo, Norway). The sodium chloride and calcium chloride used was all of analytical grade and provided by Merck (Whitehouse Station, NJ, USA) and ethylenetriaminetetraacetic acid (EDTA) by BDH Prolabo®, VWR (Oslo, Norway). The deionized water used was Milli-Q ultra pure water, with a conductivity measured at 0.7 µS.

For the protein binding experiments, the human myeloma cell RPMI-8226 (American Type Culture Collection, Rockville, MD, USA) was used. The cells were grown in RPMI 1640 (Gibco, Paisley, UK) supplemented with L-glutamine (100 µg/ml) and gentamicin (20 µg/ml), with 20 % Fetal Calf Serum (FCS). The medium was replenished twice weekly and the cells were cultured at 37 $^{o}$C in a humidified atmosphere with 5 % $CO_2$. The proteins used were Recombinant Human HGF by R&D Systems® (Minneapolis, MN, USA) and $Fc^-$ hOPG from Amgen (Thousand Oaks, CA, USA). Heparin LEO® ($M_w$ 12-15 kDa) provided by LEO Pharma (Ballerup, Denmark) was used for all protein-binding and anticoagulation experiments. The antibodies used were 10 µg/ml solutions of Primary HGF Antibody 2B5 $IgG_1$ (Deparment of cancer research and molecular medicine, NTNU, Trondheim, Norway), Human Osteoprotegerin/TNFRSF11B MAb, Mouse IgG2A from R&D Systems® and Mouse $IgG_1$ pure for primary labeling. Goat-anti-mouse (GAM) FITC Antibody was used for all secondary labeling and was purchased from BD Biosciences (San Jose, CA, USA). The HEPTEST® kit was used in the anticoagulation assay, provided by American Diagnostica Inc. (Stamford, CT, USA).

## 2.2 C5 Epimerization

Poly-M (4 g) was dissolved in deionized water. A buffer solution containing 50 mM MOPS at pH 6.9 with 2.5 mM $CaCl_2$ and 10 mM NaCl was added to the poly-M solution and preheated for one hour at 37 $^{o}$C before adding 30 mg AlgE4 enzyme dissolved in deionized water. The epimerization proceeded at 37 $^{o}$C for 48 hours under stirring before the reaction was terminated by adding a 50 mM EDTA solution. The alginate was dialyzed and freeze dried.

End-point analysis of the poly-M reference and the epimerized sample were recorded at 90 $^{o}$C on a Bruker Avance DPX 300 MHz spectrometer equipped with 5 mm QNP probe. The spectra were recorded, processed and analyzed using the software TopSpin versions 2.1 and 3.0. The alginate samples were dissolved in $D_2O$ with 5 µl 1 % trimethylsilyl propionate (TSP) as reference.

## 2.3 Acid Hydrolysis

Poly-M and poly-MG alginates were dissolved in deionized water and the pH was lowered to 5.6 using 0.1 M HCl. The alginate was then heated to 95 $^{o}$C for one hour, followed by immediate cooling and further lowering of the pH to 3.8. The solution was reheated to 95 $^{o}$C for 50 minutes before cooling and the pH was adjusted to 6.8. The alginate was dialyzed and finally freeze dried.

## 2.4 Sulfation of Alginates

Three poly-M samples were sulfated using chlorosulfonic acid concentrations of 2 %, 5 % and 10 %. For the three poly-MG samples, $ClSO_3H$ concentrations of 1 %, 2 % and 5 % were used due to the higher solubility associated with the alternating sequence. $ClSO_3H$ was added to formamide, giving a total reaction volume of 40 ml. Hydrolyzed dry alginate (1 g) was then added to each sample, and the reaction proceeded at 60 $^{o}$C for 4 hours. The alginate was precipitated from the mixture by adding 180 ml acetone and was centrifuged for 6 minutes at 5000 rpm (5810 g) on a Beckman Coulter Allegra® X-15R centrifuge. Water was added to the suspension and the pH was adjusted to 7.0 to dissolve the alginate. The pH of the solution was then lowered to 3.0 to de-ionize the alginate, followed by dialysis to remove excess ions and formamide. The pH was finally raised back to 7.0 and the alginate was freeze dried.

## 2.5 Purification of Sulfated Alginates

In order to remove traces of lipopolysaccharides (LPS) from the alginate, all samples were purified using Millistak+® Depth Filters in µPod™ format CR40 with cellulose fiber media combined with activated carbon, provided by Millipore (Billerica, MA, USA). The tubing was sterilized by rinsing with 0.1 NaOH and water, and the filters were rinsed extensively with water and 0.1 M HCl to remove carbon residues and excess ions. Alginate solutions of 500 mg dissolved in 100 ml deionized water were pumped through the filter at a rate of 15 ml/min, in recirculation over night. The final filtrate was collected in a sterile container, dialyzed and freeze dried.

## 2.6 FTIR Spectroscopy

FTIR samples were prepared by mixing 15 mg ground alginate with 600 mg analytical grade KBr powder. For each sample, 100 mg of the mixture was compressed into a transparent wafer using an applied load of 10 tons. The spectra were obtained at room temperature using a Bruker Vertex 80 system, in the range 400 $cm^{-1}$ to 4000 $cm^{-1}$.

## 2.7 SEC-MALLS

Sulfated and unmodified poly-M and poly-MG samples (10 mg) were dissolved in 1 ml deionized water and sterile filtrated through a 0.22 µm Millipore filter unit prior to SEC-MALLS. Measurements were carried out on a HPLC system consisting of a Degasys DG-1210 degasser by Dionex, together with an LC-10AD pump and an SCL-10A VP auto-injector by Shimadzu. The column used was connected to a Dawn Heleos II light scattering detector and an Optilab T-rEx RI detector, both by Wyatt Technology Corporation (Santa Barbara, CA, USA).

A refractive index (dn/dc) of 0.15 ml/g was employed for all analyzed samples, and the data were recorded and processed using the software Astra (version 4.90.07), by Wyatt Technology Corporation.

## 2.8 Elemental Analysis

The sulfur contents of the sulfated alginate samples were analyzed through high-resolution inductively coupled plasma mass spectrometry (HR-ICP-MS) at the Institute of chemistry, NTNU, by Syverin Lierhagen. Samples were prepared by dissolving 5 mg of dried alginate in 0.1 M $HNO_3$ (45 ml). The measured sulfur content was used to estimate the degree of sulfation (DS), defined as the average number of sulfate groups per alginate monomer, through the following mass-balance equation where x represents the DS:

$$C_6O_6H_5 + (x+1)Na^+ + xSO_3^- + H_2O = Total\ monomer\ mass \qquad (2.1)$$

It was assumed in equation 2.1 that approximately 10 % water was associated with the alginate and one sodium counter-ion with each negative charge. DS values were plotted against the corresponding theoretical sulfur content, creating the standard curve shown in Appendix B. A second degree function was fitted to the curve, and the DS values corresponding to the measured sulfur content of the sulfated alginate samples were calculated.

## 2.9 $^{13}$C NMR Analysis

All $^{13}$C NMR spectra were recorded at 40 $^{o}$C on a NMR Bruker Avance 600 MHz spectrometer equipped with a z-gradient CP-TCI probe. The spectra were recorded, processed and analyzed using the software TopSpin versions 2.1 and 3.0. The alginate samples were dissolved in $D_2O$ with 5 µl 1 % trimethylsilyl propionate (TSP) as reference. The$^{13}$C NMR spectra were recorded using an inverse gated decoupling pulse scheme with a 30° flip angle and 5 seconds intrascan delay. Signal assignations were made through the employment of multi-dimensional NMR techniques, by Finn L. Aachmann at the Department of biotechnology, NTNU. Estimations of the sulfation degrees (DS) for the sulfated poly-M samples were made by integrating the signals and calculating the area fraction of peaks raised from sulfated carbons C2 and C3 through, as shown in equation 2.2.

$$DS = (I_{2S} + I_{3S})/(I_{2S} + I_{3S} + I_2 + I_3) \qquad (2.2)$$

The DS was also estimated with respect to C1, by calculating the fraction of signals associated with monosubstituted (S) and disubstituted monomers (SS) relative to the total integrated C1 signals, as shown in equation 2.3.

$$DS = (I_S + I_{SS})/(I_S + I_{SS} + I_1) \qquad (2.3)$$

## 2.10 Inhibition of Cell Surface Protein Binding

### 2.10.1 Hepatocyte Growth Factor (HGF)

Stock solutions of sulfated alginates were prepared by dissolving 10 mg alginate in 0.5 ml deionized water and sterile filtration of the solutions using a 0.22 µm Millipore filter unit. Myeloma RPMI cells were incubated in a 1 µg/ml solution of HGF in sterile phosphate buffered saline (PBS) with 0.1 % bovine serum albumin (BSA), for 15 minutes. The cells were stimulated for 10 minutes using increasing concentrations of heparin or sulfated alginates (0.001-10 µg/ml), as well as high-concentration samples of the non-sulfated poly-M and poly-MG alginates (3 and 10 µg/ml), diluted in 100 µl PBS/0.1 % BSA. HGF antibody (Ab) 2B5 was added to samples stimulated with HGF, while an isotype control sample was labeled with Mouse $IgG_1$ pure Ab for 25 minutes. Secondary labeling was performed by adding GAM FITC Ab to all samples, followed by incubation for another 25 minutes. The cells were finally re-suspended in PBS. All samples were washed with 2 ml of a PBS/0.1 % BSA solution and centrifuged between each incubation step.

### 2.10.2 Osteoprotegerin (OPG)

Myeloma RPMI cells were incubated with 5 µg/ml OPG in sterile PBS/0.1 % BSA for 15 minutes and stimulated with a single concentration (3 µg/ml) of heparin, sulfated alginates and unmodified poly-M and poly-MG alginates. The cells were labeled using Human OPG MAb followed by GAM FITC Ab following the same protocol as described above for HGF.

Fluorescing antibody-labeled cells were detected by flow cytometry using a FACS-LSRII instrument, by BD, and the data were recorded and subsequently analyzed using the flow cytometry analysis software FlowJo (Tree Star, Ashland, OR).

## 2.11 *In vitro* Measurement of Plasma Coagulation Time

Anticoagulant properties of the sulfated alginates were studied using the HEPTEST® assay, measuring the increase in normal human plasma (NHP) coagulation time as a function of factor Xa inactivation. The selected dose range of heparin was 1.7-13.9 µg/ml while a range of 7.0-222.4 µg/ml was chosen for the sulfated alginates based on initial experiments. Heparin or sulfated alginate samples diluted in NHP (100 µl) were heated to 37 $^{o}$C in plastic flow tubes. Factor Xa reconstituted in distilled water (100 µl) at 25 $^{o}$C was added to the samples, followed by 100 µl RECALMIX, in accordance with the HEPTEST - HI ASSAY protocol. The time from added RECALMIX to observed solidification of the plasma was recorded.

# 3 Results

## 3.1 C5 Epimerization of Polymannuronic Acid

Polymannuronic acid (poly-M) was epimerized using the C5 epimerase AlgE4. The $^{1}H$ spectra of the poly-M template and the resulting epimerization product are shown in Figure 9.

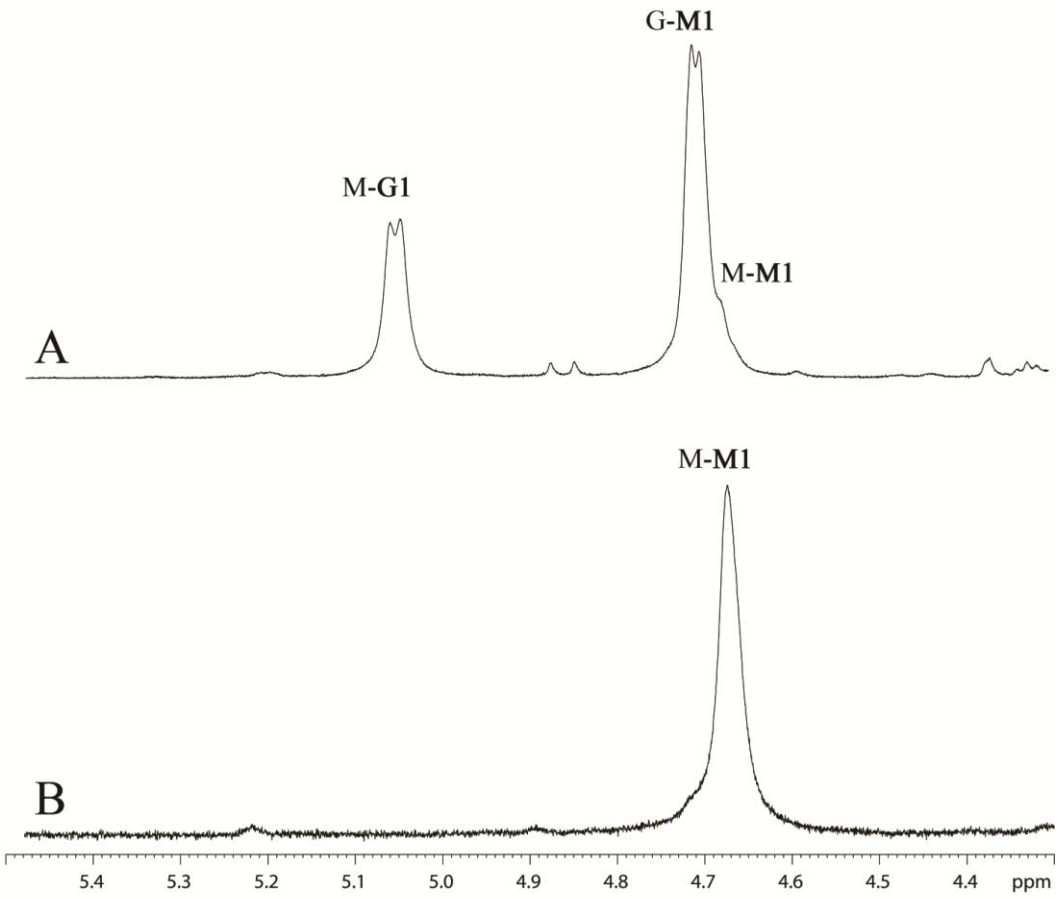


**Figure 9: $^{1}H$ NMR spectra of the anomeric regions of the (A) epimerization product after epimerization of (B) polymannuronic acid, with AlgE4. The assignation marks protons associated with carbon 1 of mannuronic acid or guluronic acid, along with the identity of the adjacent monomer. Samples were dissolved in $D_2O$ and recorded on a 300 MHz spectrometer at 90 $^{o}C$.**

Spectrum B showed a novel peak at approximately 5.1 ppm, which was assigned to the anomeric proton of C1 on α-L-guluronic acid. The anomeric M-**M1** signal in the polymannuronic acid, at approximately 4.65 ppm, had diminished noticeably, appearing as a shoulder on the adjacent G-**M1** peak risen in spectrum A of Figure 9. Integration of the anomeric proton signals observed at ~4.7 ppm for β-D-mannuronic acid and ~5.1 ppm for α-L-guluronic acid showed a guluronic acid fraction ($F_G$) of 0.46 in spectrum B. From the epimerization pattern of AlgE4 previously described and the resulting $F_G$, the epimerization product was designated as an alginate containing almost exclusively MG-blocks (poly-MG).

## 3.2 FTIR Spectroscopy

FTIR spectral data for sulfated poly-M and poly-MG samples are presented in Figure 10 and Figure 11. Compared with the unmodified M and MG samples, new peaks were observed respectively at 1260 $cm^{-1}$ and 1250 $cm^{-1}$ for the sulfated derivatives, attributed to asymmetrical S=O stretching (Fan, Jiang et al. 2011). The transmittance values of this peak were approximately equal for the 10 % S-M and 5 % S-M samples shown in Figure 10, while a lower intensity was observed in the same peak for the 2 % S-M sample.

A similar pattern was observed in the MG spectra shown in Figure 11, where the most prominent S=O peak was observed in the 5 % S-MG sample. The same peak of the 2 % S-MG curve showed a weaker intensity compared to the 1 % S-MG sample. The former sample did, however, exhibit a weaker signal along the whole spectrum with lower recorded transmittance values at the referential alginate peaks as well. As the transmittance is correlated to molecular concentration in the sample, the result indicated a lower alginate concentration in the prepared wafer relative to the other samples.

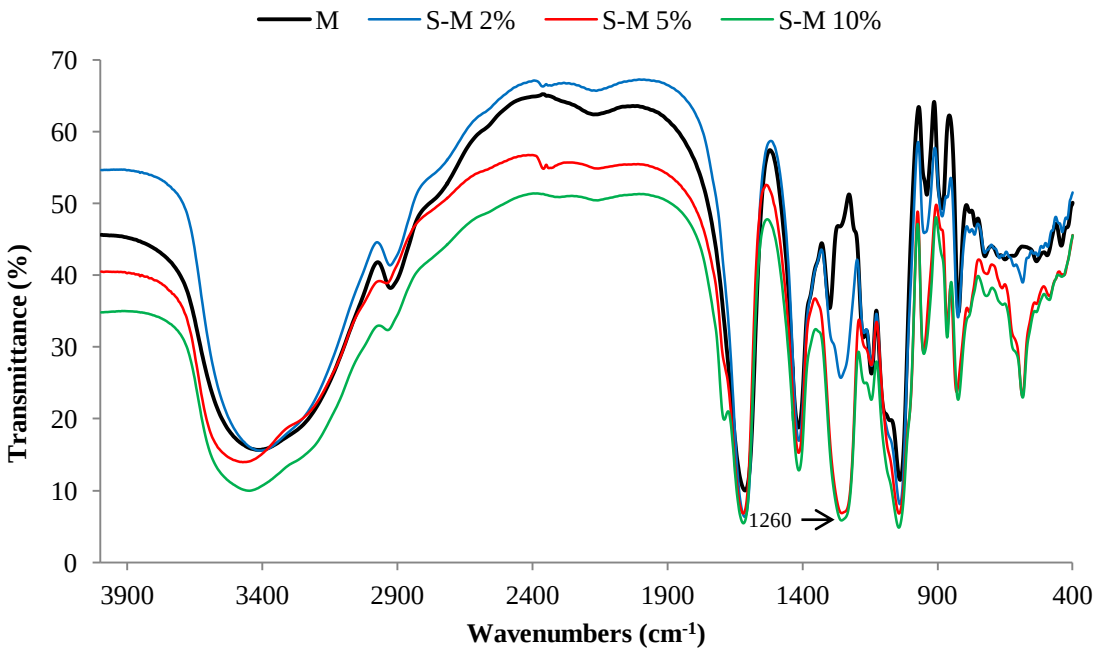


**Figure 10: FTIR transmission spectra of solid KBr pellet samples of poly-M alginates; unmodified (M) and sulfated (S-M) using chlorosulfonic acid concentrations of 2 %, 5 % and 10 %. The spectra were recorded at room temperature.**

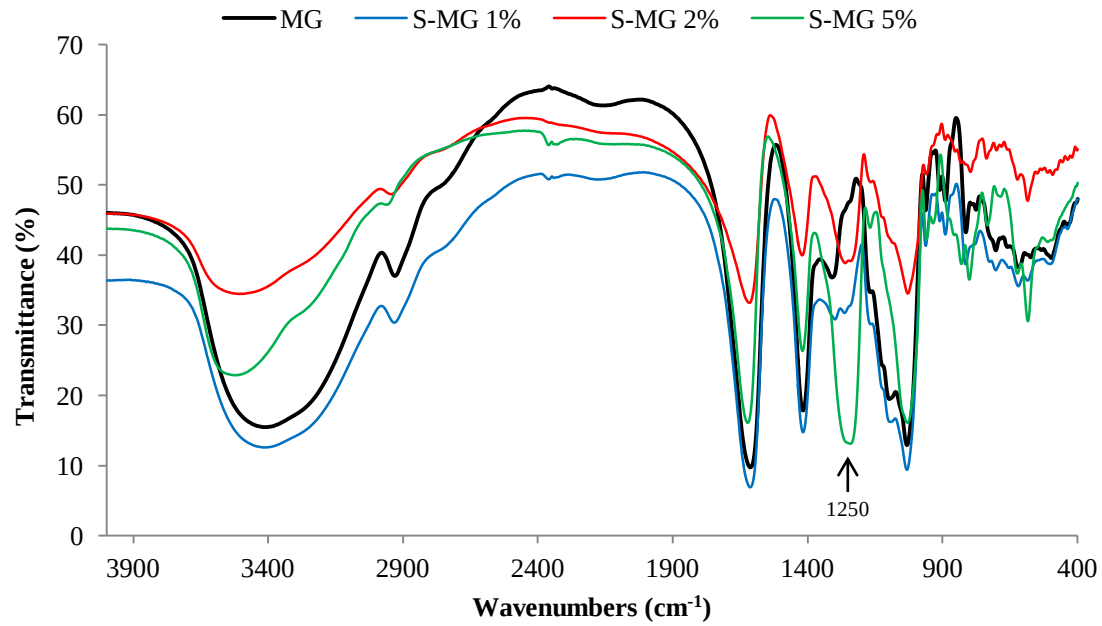


**Figure 11: FTIR transmission spectra of solid KBr pellet samples of poly-MG alginates; unmodified (MG) and sulfated (S-MG) using chlorosulfonic concentrations of 1 %, 2 % and 5 %. The spectra were recorded at room temperature.**

An additional novel peak was observed at approximately 600 $cm^{-1}$ in all the sulfated alginates, most prominently shown in Figure 10. The peak could not be assigned with confidence due to the low resolution in the frequency region, but was presumed to have risen from the attached sulfate group rather than sample impurities, due to a transmittance shift pattern similar to that of the S=O peaks observed at 1250 and 1260 $cm^{-1}$ in the figures above.

## 3.3 SEC-MALLS

The molecular weight averages and distributions of the sulfated alginate samples as well as the unmodified poly-M and poly-MG alginates were studied using SEC-MALLS. The measured weight and number averages, corresponding DP estimations and polydispersity values are shown below in Table 1, and the mass distributions are shown Figure A 1 and Figure A 2 in Appendix A.

**Table 1: SEC-MALLS data for poly-M and poly-MG alginates sulfated using chlorosulfonic acid concentrations of 1 %, 2 %, 5 % and 10 % compared with unmodified (M and MG) alginates. Mn = Molecular number average, Mw = Molecular weight average, DP = Degree of polymerization.**

| Sample | $M_n$ (kDa) | $M_w$ (kDa) | Polydispersity | DP |
|---|---|---|---|---|
| **Poly-M** | 23.8 | 32.1 | 1.35 | 120 |
| **2 % S-M** | 23.0 | 30.6 | 1.33 | 116 |
| **5 % S-M** | 22.1 | 31.4 | 1.43 | 112 |
| **10 % S-M** | 24.2 | 32.6 | 1.35 | 122 |
| **Poly-MG** | 11.8 | 14.3 | 1.21 | 60 |
| **1 % S-MG** | 12.1 | 17.0 | 1.41 | 61 |
| **2 % S-MG** | 12.8 | 18.4 | 1.43 | 65 |
| **5 % S-MG** | 15.8 | 22.9 | 1.45 | 80 |

The calculated weight averages of all the poly-M samples were found to be approximately twice that of the poly-MG samples, while a relatively small difference in molecular weight was observed within the samples of each alginate type. For poly-MG, higher $M_w$ and $M_n$ values were associated with increasing concentration of the sulfating reagent used. A similar tendency was observed in the molecular weight average of the sulfated poly-M samples, but the unmodified alginate showed a higher value than two of the sulfated samples, and no direct relationship was observed between the sulfating conditions and the molecular number average of the poly-M samples.

The chromatography curves depicted in Appendix A showed no apparent change in the mass distribution of the poly-MG samples as a result of the sulfation reaction. A small shift was observed in the sulfated poly-M samples compared to the unmodified reference sample, where the 5 % S-M and 10 % S-M samples exhibited slightly longer elution time, suggesting a minor degree of degradation. The low amplitude of the S-MG curves was assumed to be caused by a lower alginate concentration in the prepared samples.

## 3.4 Elemental Analysis

The sulfur contents of the sulfated alginate samples were measured through elemental analysis using HR-ICP-MS and are shown below in Table 2 along with the corresponding estimations of the degrees of sulfation (DS). The calculation of DS is elaborated in Appendix B. For the sulfated poly-MG samples, the DS values increased with the concentration of the sulfating reagent used, where the 5 % S-MG sample showed the highest sulfate content with an average of 1.08 sulfate groups per monomer. The highest estimated DS in the poly-M samples was attained when using a concentration of 5 % chlorosulfonic acid, with 0.87 sulfate groups per monomer. When doubling the concentration of the sulfating reagent in the 10 % S-M sample, a decrease of the DS was observed.

**Table 2: Measured sulfur contents and estimated degrees of sulfation (DS) of poly-M and poly-MG alginates, sulfated using chlorosulfonic acid concentrations of 1 %, 2 %, 5 % and 10 %, from elemental analysis using high resolution ICP-MS.**

| Sample | Sulfur content (µg/g) | Sulfur content (%) | DS |
|---|---|---|---|
| **2 % S-M** | 16 124 | 1.61 | 0.12 |
| **5 % S-M** | 91 359 | 9.14 | 0.87 |
| **10 % S-M** | 82 222 | 8.22 | 0.76 |
| **1 % S-MG** | 10 774 | 1.08 | 0.08 |
| **2 % S-MG** | 60 921 | 6.09 | 0.53 |
| **5 % S-MG** | 106 993 | 10.70 | 1.08 |

Only a small amount of sulfur was detected in the 2 % S-M and the 1 % S-MG samples, resulting in the lowest calculated DS values. It was observed that the 2 % S-M sample failed to dissolve completely in the $HNO_3$ prior to analysis.

## 3.5 $^{13}$C NMR Analysis

The sulfation degrees and substitution patterns of the sulfated alginate samples were studied using $^{13}$C NMR with unmodified poly-M and poly-MG alginates as reference spectra. The spectra of the sulfated alginates revealed new peaks originating from carbon atoms directly attached to sulfate group and indirectly from adjacent carbons through coupling mechanisms. The recorded spectra of poly-M and its sulfated derivatives are shown in Figure 12 with proposed peak assignation.

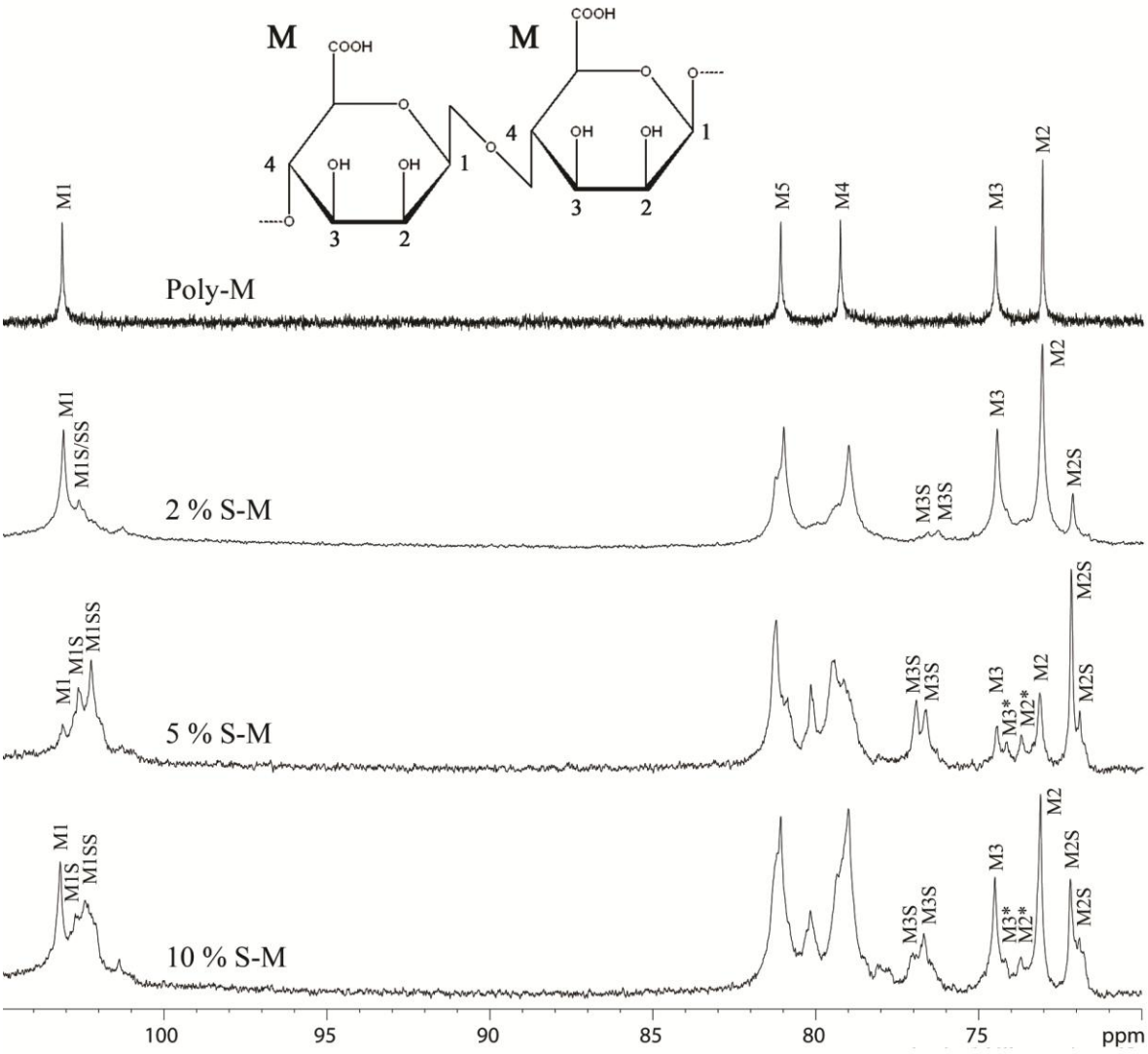


**Figure 12: $^{13}C$ NMR spectra of unmodified poly-M and sulfated poly-M (S-M) alginates using chlorosulfonic acid concentrations of 2 %, 5 % and 10 %. S = monosulfated monomer, SS = disulfated monomer, * = unmodified monomer adjacent to sulfated monomer. Samples were dissolved in $D_2O$ and the spectra were recorded at 40 $^oC$ on a 600 MHz spectrometer with an inverse gated decoupling scheme, 30$^o$ pulse angle and 5 seconds intrascan delay.**

A diverging of the anomeric carbon signal (M1) at approximately 103 ppm was observed as a result of the sulfation. The 5 % S-M spectrum in particular showed two prominent peaks at a lower resonance frequency than the unmodified C1 signal, where the least intense peak was proposed to arise from C1 on a mannuronic acid monomer where only C2 was sulfated, while the adjacent peak at the lower resonance frequency was assigned to C1 of an M unit where both C2 and C3 were sulfated.

Novel peaks in the 78-82 ppm region of the sulfated alginates were not readily distinguishable, and as they were not directly relevant for the DS estimations, the signals were collectively assigned as derivative signals of C4 and C5. A distinct shift to a higher resonance frequency was observed in the sulfated C3 peak of mannuronic acid (M3S), which appeared at approximately 77 ppm, with the adjacent C3 signal representing a disulfated monomer. The most distinguished newly formed peak was that proposed as the sulfated C2 carbon found at 72 ppm, at a lower resonance frequency than the unmodified C2. In the 5 % S-M and 10 % S-M spectra, an adjacent peak of lower intensity was observed at a lower frequency than the M2S signal, assigned to C2 on a disulfated M unit.

Estimations of the degrees of sulfation for the samples were made through integration of the signals with respect to C1 or C2 and C3, and are shown below in Table 3.The signals assigned to monosulfated and disulfated monomers were included in the same integral when calculating the DS. Integration of the C1 signals resulted in DS estimations 18 %, 27 % and 35 % higher than the estimations based on C2/C3 integration for the 2 % S-M, 5 % S-M and 10 % S-M samples, respectively. The integration values used for the calculations are listed in Appendix C.

**Table 3: Estimated degrees of sulfation of poly-M alginates sulfated using chlorosulfonic acid concentrations of 2 %, 5 % or 10 %, based on integration of $^{13}$C NMR signals of either C1 or C2 and C3. Integration values are listed in Appendix C.**

| Sample | DS (C1) | DS (C2/C3) |
|---|---|---|
| **2 % S-M** | 0.38 | 0.21 |
| **5 % S-M** | 0.89 | 0.70 |
| **10 % S-M** | 0.69 | 0.51 |

The $^{13}$C spectra of poly-MG and its sulfated derivatives are shown in Figure 13 with assignation for the unmodified alginate sample.

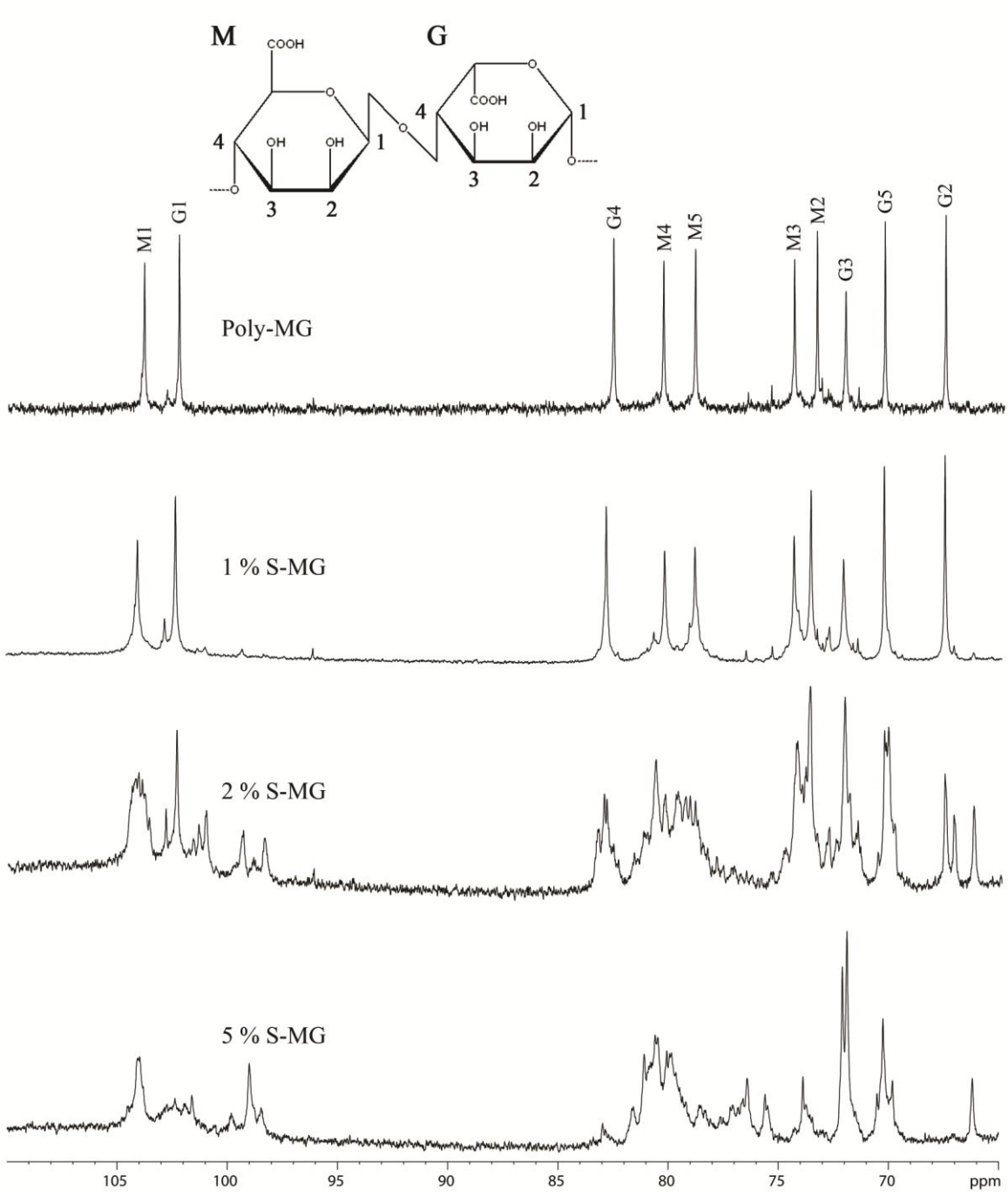


**Figure 13: $^{13}$C NMR spectra of unmodified poly-MG and sulfated poly-MG (S-MG) alginates using chlorosulfonic acid concentrations of 1 %, 2 % and 5 %. Samples were dissolved in $D_2O$ and the spectra were recorded at 40 $^{o}$C on a 600 MHz spectrometer with an inverse gated decoupling scheme, 30$^{o}$ pulse angle and 5 seconds intrascan delay.**

Sulfation of the poly-MG samples resulted in more complex NMR spectra compared with poly-M. The relatively low sulfation degree of the 1 % S-MG sample estimated from elemental analysis was reflected in a spectrum similar to that of the unmodified poly-MG. For the 2 % S-MG and 5 % S-MG samples, a large diverging of the signals particularly

associated with C4 of the M and G monomers and C5 of M was observed. The intensity of the G2 signal was visibly reduced in the 2 % S-MG, while two new peaks appeared at a lower resonance frequency. The G2 peak was not observed at all in the 5 % S-MG spectrum, and only one peak at approximately 66 ppm was observed at a lower resonance frequency relative to G2. The G3 signal at 72 ppm did not decrease noticeably as a result of sulfation, while a split signal was observed in the 5 % S-MG sample at the same resonance frequency. In the C1 region an amplification of the signals in the 98-101 ppm region was observed, while the G1 signal was greatly reduced in the 5 % S-MG sample, as seen with the G2 peak. The M2 and M3 signals were relatively unchanged from the poly-MG reference in the 1 % S-MG and 2 % S-MG, although some apparent splitting of the signals had occurred in the latter sample. Both signals diminished notably in the 5 % S-MG sample, and shifts of the M2 and M3 peaks to different resonance frequencies were observed.

## 3.6 Inhibition of Cell Surface Protein Binding

Hepatocyte growth factor (HGF) and osteoprotegerin (OPG) have previously been shown to bind heparin, and were in the present study evaluated for their ability to bind sulfated alginates. Human myeloma RPMI cells were incubated with HGF or OPG and treated with heparin or sulfated alginates to release the proteins from the cell surface. Following treatment, the proteins were labeled with fluorescent antibodies and flow cytometry was employed to measure the mean fluorescence (MFI) of the cell samples, corresponding to the amount of remaining cell-bound proteins. A protein-stimulated, untreated cell sample was used as negative control, while the isotype control sample was treated with a primary antibody unable to bind HGF or OPG, thus serving as a positive control. The sulfated alginates 2 % S-MG, 5 % S-MG, 5 % S-M and 10 % S-M were shown to be the most potent samples in initial experiments (Figure D 2, Appendix D), and were selected for all proceeding protein binding experiments as well as the anticoagulation assay later described.

### 3.6.1 Hepatocyte Growth Factor (HGF)

The HGF-stimulated untreated sample was used as negative control equivalent to 100 % cell-bound HGF at zero treatment concentration set to 0.0001 µg/ml. The measured mean MFI values (Table D 1, Appendix D) for all samples were related to the negative control and graphed as percent cell-bound HGF as a function of treatment concentration, as shown in Figure 14, with guidance lines showing the proposed dose-response curve.

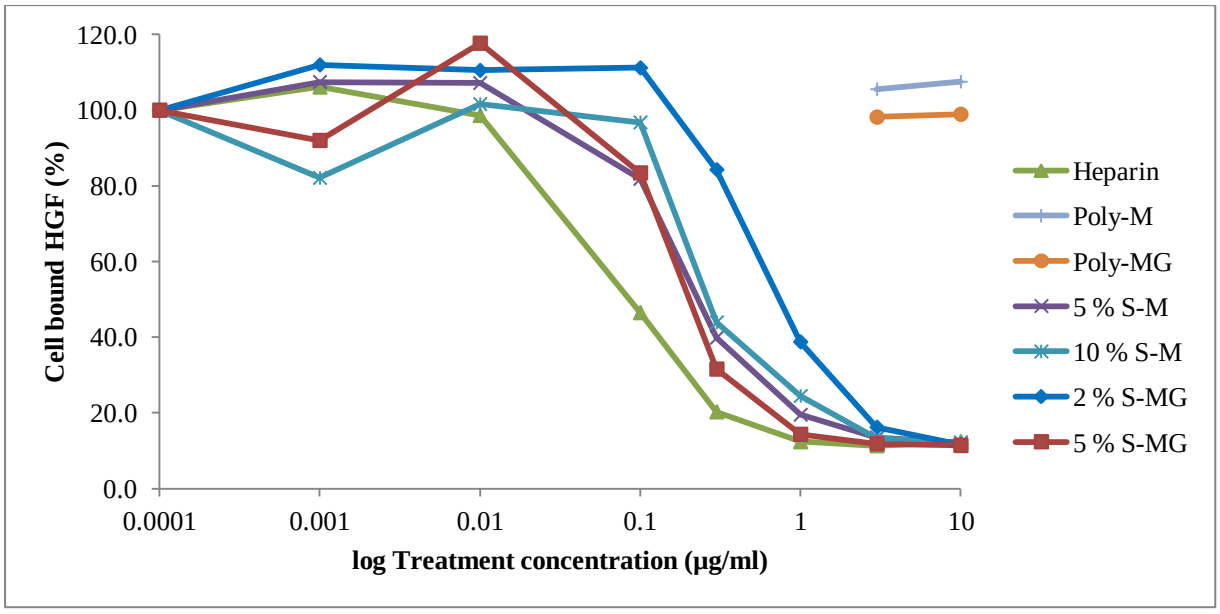


**Figure 14: Release of HGF from myeloma RPMI cell surface by treatment with heparin or poly-M and poly-MG alginates either unmodified or sulfated using chlorosulfonic acid concentrations of 2 %, 5 % and 10 %, as a function of treatment concentration. Mean fluorescence intensities were recorded by flow cytometry and converted to percent cell-bound HGF in reference to the untreated control sample. The S-M and S-MG samples were tested in separate experiments.**

A dose dependency was observed for the effect of heparin and sulfated alginate species used, where maximal HGF releasing occurred around 3 µg/ml treatment concentration for all samples as the MFI values approached that of the positive control sample. When using a dose of 0.01 µg/ml, neither of the samples showed any appreciable reduction in cell-bound HGF, indicating a thinning out of the measured effect. The apparent decrease in cell-bound HGF at a treatment concentration of 0.001 µg/ml for 5 % S-MG and 10 % S-M was assumed to be caused by inadequate sample preparation as the aberration was not observed in repeated experiments.

To evaluate the relative efficacy of the samples within the response window, the inhibitory concentration at 50 % cell-bound HGF ($IC_{50}$) was studied. At this value heparin showed to be the most efficacious and retained high protein binding activity at 0.1 µg/ml treatment concentration, while 5 % S-M, 10 % S-M and 5 % S-MG showed a relatively similar impact where the effect was nearly thinned out at the same concentration. Of all the tested samples in the current experiment, 2 % S-MG was the least effective in displacing HGF from the cell surface, as the amount of cell-bound protein diminished noticeably when lowering the treatment concentration from 1 µg/ml to 0.3 µg/ml. As an additional control, treatments of non-sulfated poly-M and poly-MG alginates were tested at concentrations of 3 µg/ml and 10 µg/ml. All four of the unmodified samples showed MFI values similar to that of the negative control, indicating that no measureable HGF binding and release from the cells had occurred as a result of the treatments, despite the high doses.

### 3.6.2 Osteoprotegerin (OPG)

An OPG-stimulated untreated sample was used as a negative control, while the isotype control labeled with a non-binding primary antibody was set as a positive control in the experiment. Measured MFI values from flow cytrometry were converted to percent cell-bound OPG in relation to the negative control (Table D 3, Appendix D), and the results of the experiment are shown in Figure 15. A concentration of 3 µg/ml was used for all treatments.

Using non-sulfated poly-M and poly-MG alginates resulted in no appreciable release of OPG from the cell surface, with recorded MFI values equivalent to that of the untreated sample. Heparin and the four sulfated alginate samples used showed an almost equal effect at the given treatment concentration, although none reached the limit value of the positive control, as was observed in the HGF-binding experiment.

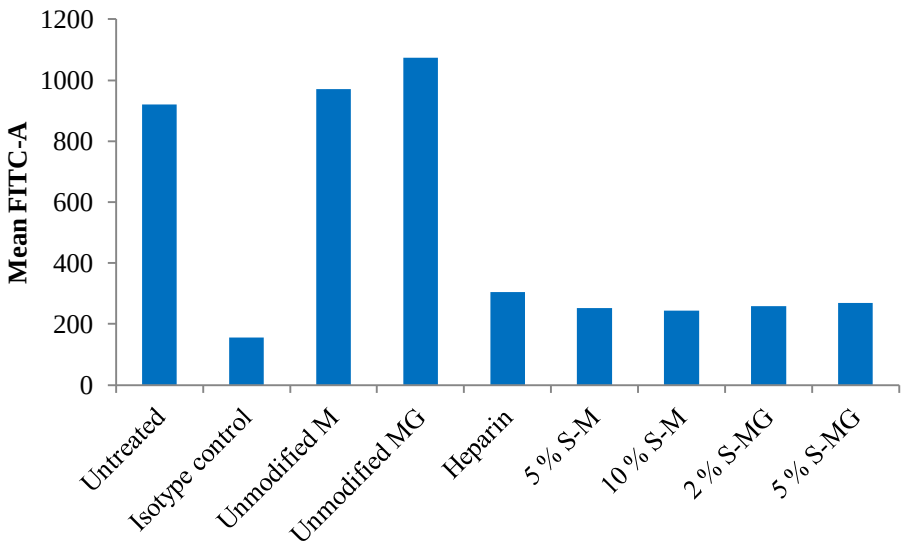


**Figure 15.: Release of OPG bound to myeloma RPMI cell surfaces through treatment with 3 µg/ml solutions of heparin and poly-M and poly-MG alginates either unmodified or sulfated using chlorosulfonic acid concentrations of 2 %, 5 % or 10 %. Mean fluorescence intensities were recorded by flow cytometry and converted to percent cell-bound OPG in reference to the untreated control sample.**

## 3.7 *In vitro* Measurement of Coagulation Time

Increasing doses of heparin (1.7-13.9 µg/ml) and sulfated alginates (7.0-222.4 µg/ml) were added to normal human plasma followed by supplementation of factor Xa, and the time required for visible coagulation was recorded. A pure plasma sample with factor Xa was set as a zero concentration negative control. The resulting plasma coagulation times from sulfated alginate and heparin treatments are graphed below in Figure 16 and Figure 17, respectively, with guidance lines representing the proposed dose-response curves. Concentrations used and the corresponding coagulation times in seconds are listed in Appendix E.

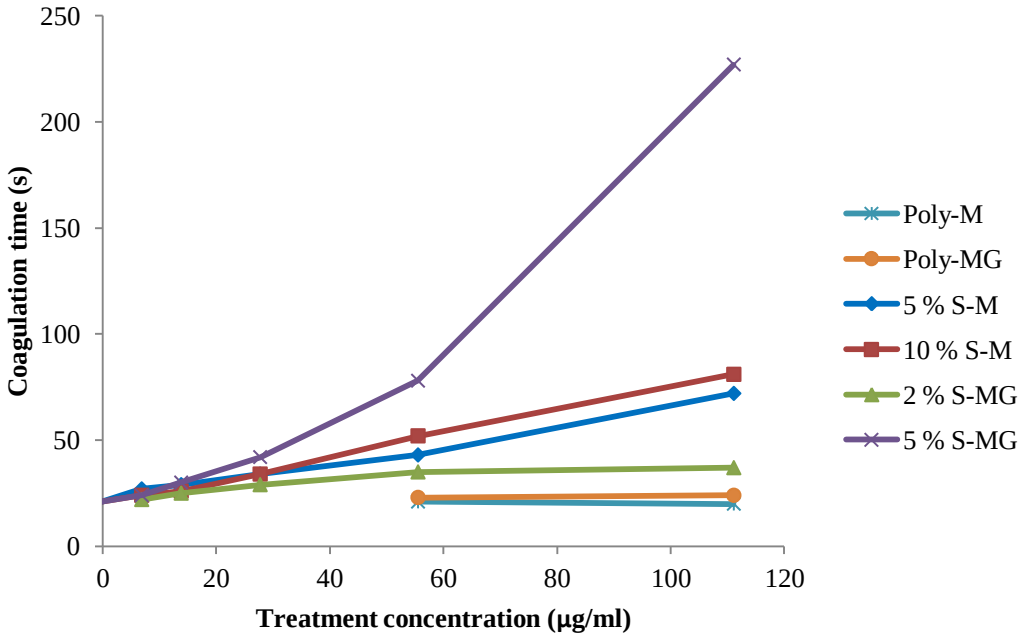


**Figure 16: Recorded coagulation times (s) of normal human plasma supplemented with factor Xa and treated with poly-M and poly-MG alginates either unmodified or sulfated using chlorosulfonic acid concentrations of 2 %, 5 % or 10 %, as a function of treatment concentration.**

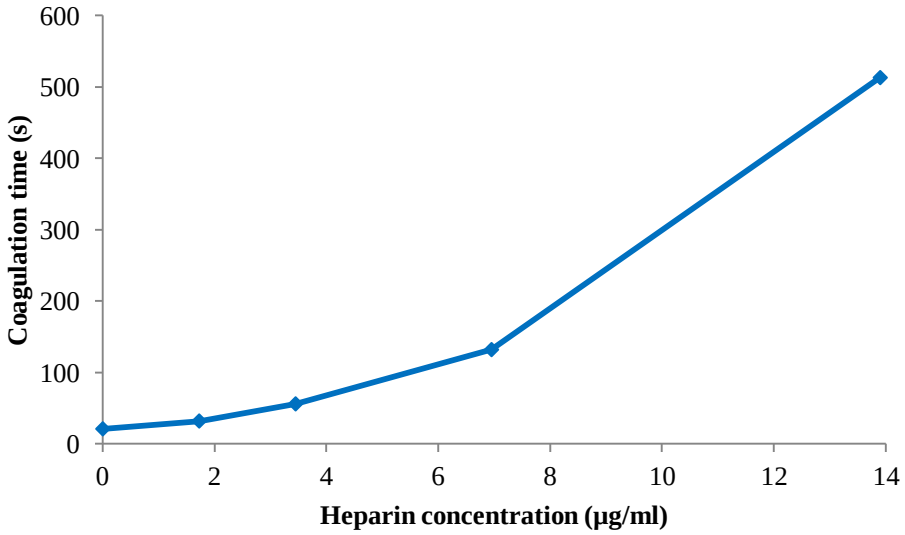


**Figure 17: Coagulatime time (s) of normal human plasma supplemented with factor Xa and treated with heparin as a function of heparin concentration.**

A higher concentration of the sulfated alginate samples was required to appreciably increase the coagulation time of the plasma in comparison with heparin. For the 2 % S-MG and both S-M samples, a steady non-proportional rise in the coagulation time was observed with increasing sample concentrations, while the plasma samples treated with 5 % S-MG showed a steeper exponential-like increase in coagulation time within the dose range, similar to that of heparin shown in Figure 17. When the concentration was increased to 222 µg/ml (not shown), coagulation was achieved only in the 2 % S-MG (41 seconds), while the remaining samples failed to coagulate after 10 minutes had passed. To evaluate the effect of sulfation, unmodified poly-M and poly-MG alginates were studied in parallel at concentrations of 56 µg/ml and 111 µg/ml. Treatment with non-sulfated poly-M and poly-MG alginates showed no measurable effect on the plasma coagulation, with recorded times equivalent to that of the negative control sample (21 s).

An earlier coagulation experiment performed under the same conditions, but using plasma from a different donor, showed the same relative efficacy between the sulfated alginate samples. However, a steep increase in coagulation time was seen at 56 µg/ml for the 5 % and 10 % S-M samples, similar to that of 5 % S-MG at 111 µg/ml shown in the results above. Treatment with the 2 % S-MG sample showed the same result in both experiments, exhibiting a slow, linear increase in coagulation time as a function of treatment concentration.

# 4 Discussion

Chemical sulfation of poly-M and poly-MG alginates was successfully achieved, evident in the elevated sulfur content measured through elemental analysis and the appearance of a novel FTIR peak corresponding to the S=O double bond of a sulfate group. While not quantifiable due to some sample concentration differences, the FTIR spectra showed the bond present in all sulfated alginate samples and absent in the poly-M and poly-MG reference curves. The carbon NMR spectra revealed several new peaks with signal intensities strongly affected by the chlorosulfonic acid concentration used for sulfation. The most prominent changes in the NMR spectra were associated with C2 and C3, indicating a modification occurrence at these carbons. Furthermore, no significant amounts of reaction by-products or other impurities were observed when interpreting the NMR spectra, indicating that the samples were sufficiently purified following sulfation.

Although a clear effect was seen of increasing the chlorosulfonic acid concentration on the resulting degrees of sulfation estimated by elemental analysis, no direct relationship was shown. One of the reasons for the unpredictable response observed may have been partial precipitation of the alginate due to the acidic conditions of the sulfation reaction. The solubility of the alginate is dependent on the acid strength as well as alginate sequence and molecular weight, which resulted in varying degrees of precipitation between the samples used, particularly for the poly-M samples. There was no visible precipitation of the poly-MG during the reaction, resulting in a somewhat more predicted response with regard to the estimated sulfation degrees, where the DS value increased with the concentration of the chlorosulfonic acid used. Precipitation may shield parts of the polymer towards the surrounding acid and decrease degradation, but it also lowers the exposure to the sulfating reagent and may thus limit the maximal sulfation degree. Partial precipitation of the alginates would also be expected to result in heterogeneous sulfation patterns, as parts of the alginate would be unexposed to the sulfating reagent. Conversely, homogenous sulfation, with random sulfate distribution along the whole length of the polysaccharide chain, would have been expected with a fully dissolved and exposed alginate. Although not apparent due the complexity of the sulfated poly-MG $^{13}C$ NMR spectra, it is reasonable to expect that a more homogenous sulfation of the poly-MG alginates occurred as a result of the higher solubility observed during the sulfation reaction, compared to

poly-M. The cause of the higher solubility was assumed to be the higher flexibility of the polyalternating alginate. As the poly-MG alginate is also more prone to acidic degradation, the lower chlorosulfonic acid concentrations used (1 %, 2 %, 5 %) were favorable considering that no apparent degradation was observed from the SEC-MALLS data. The poly-M alginates were sulfated using higher chlorosulfonic acid concentrations at 2 %, 5 % and 10 %, and there were indications of some degradation in the two latter samples from the mass distribution curves shown in Appendix A. The relatively higher degradation rate of poly-MG alginates did, however, result in a lower weight average compared to the poly-M samples due to identical acid hydrolysis protocols *prior* to sulfation, which was evident when comparing $M_w$ values non-sulfated poly-M and poly-MG samples, shown in Table 1.

Considering the light scattering data for the sulfated poly-MG samples, the observed increase in $M_w$ was reasonable as an attached sulfate group adds nearly 50 % to the molecular weight of each monomer, and more if counting an additional sodium counter-ion associated with each sulfate group. On the other hand, degradation of the samples would have resulted in a decrease in $M_w$, which was neither apparent from the chromatography curves nor the measured polydispersity. It was, however, not feasible to make precise estimations of the molecular weights and DS values for the sulfated alginates based on these data, as the sulfation alters the structural characteristics of the alginate in a manner that would have required a different refractive index (dn/dc) input value. The dn/dc value would in principle also differ between varying degrees of sulfation, requiring quantification prior to SEC-MALLS and experimental determination of dn/dc. The refractive index affects the calculation of the molecular weight averages, which may have contributed to the aberrations observed in the sulfated poly-M samples. The obtained SEC-MALLS data were still valid for comparing the weight average of the unmodified poly-M and poly-MG samples as well as the polydispersity of all samples, which is independent of dn/dc.

The NMR spectra of all the sulfated poly-M samples showed a greater intensity of the signals assigned to C2 of the single-sulfated monomer (M2S) compared to the equivalent peak of C3 (M3S) (Figure 12). This observation indicated a substitution preference most likely to be caused by steric hindrance from the alginate's conformation towards the relatively bulky sulfate group. There were, however, distinguished signals showing

substitution of both C2 and C3 on a single mannuronic acid monomer, enabling utilization of both sulfation sites simultaneously despite the apparent C2 preference. Considering that some precipitation of the alginate was observed during sulfation of the poly-M samples, partial shielding from the surrounding chlorosulfonic acid may have affected the resulting sulfation pattern.

The complexity of the sulfated poly-MG carbon spectra (Figure 13) prevented peak assignation with certainty. That would have required a sulfated poly-G reference as well as in-depth study using multidimensional NMR techniques. In addition to introducing several more peaks than in the poly-M alginates, sulfation of the poly-MG alginates also showed dissimilar shifting patterns in the resonance frequencies due to the different conformation of the alternating sequence. The disappearance of the G2 peak in the highly sulfated 5 % S-MG sample indicated a high degree of substitution at C2 of the G monomer. Considering the C1 region, a greater decrease in intensity was observed for the G1 signal compared with the adjacent M1 peak. Due to the intricate signal diverging it was not possible to identify the corresponding signals on the sulfated monomers with sufficient confidence, but the greater impact of sulfation on the G1 signal suggested a preference for substitution on the guluronic acid monomer in the current study. The diminished M2 and M3 signals in the 5 % S-MG sample did, however, indicate sulfation at these carbons as well. As the G3 signal intensity was not appreciably reduced from sulfation, the apparent signal splitting at 72 ppm was presumed to be the result of a newly formed peak corresponding to a sulfated C2 or C3 of the M monomer. The relatively low effect of the sulfation reaction on the G3 signal also indicated that C3 on the G monomer was not the primary substitution target, as was observed with M3 in the sulfated poly-M spectra.

Attempted quantification of the DS in sulfated poly-M samples through $^{13}C$ NMR resulted in non-matching DS values when integrating with respect to C1 as opposed to C2 and C3 (Table 3). Although the DS roughly corresponded to the elemental analysis data shown in Table 2, the estimations were not feasible due to the disparity of the values for each sample. Precise quantification of natural substances using carbon NMR can be challenging due to a low abundance of the $^{13}C$ isotope and because of the spin-lattice relaxation time ($T_1$) of $^{13}C$, which is typically very long compared to $^{1}H$. The long $T_1$ necessitates a long recycle delay between scans, making the whole experiments

exceedingly time-consuming. In the present study, a 5 second intrascan delay to a $30^{o}$ pulse was applied, corresponding to a pulse sequence recycle delay of approximately 15 seconds. It has been indicated that a longer recycle delay, of at least 20 seconds, is required to achieve full relaxation, and thus precise quantification from carbohydrate $^{13}C$ NMR spectra (Bubb 2003). The DS values obtained from elemental analysis were therefore considered more accurate estimates in the present study. Nonetheless, elemental analysis is, similar to quantitative FTIR analysis, highly dependent on the alginate concentration in the sample. A weaker signal was observed in the FTIR spectrum of the 2 % S-MG sample (Figure 11), indicating a lower alginate concentration despite meticulous weighing of the dried alginate samples. The aberration is likely due to the anionic character of the alginates, which can cause inclusion of salts, water and possibly other impurities in the samples, thus adding to the total dry weight. It was also observed that the 2 % S-M alginate failed to dissolve completely in $HNO_3$ during sample preparation for the elemental analysis, which may also have caused an underestimation of the actual sulfur content in the sample. Parallel measurement of the samples' carbon content for incorporation in the mass balance would have been required to achieve a more credible DS estimation from elemental analysis. Quantitative NMR is essentially independent of sample concentration, as the integration is based on the relative intensities of the signals. It would therefore be the preferred quantification tool for prospective research, provided that the sensitivity can be increased sufficiently and the peaks assigned unambiguously.

Sulfation greatly improved the HGF and OPG binding properties of the alginates when compared with the unmodified poly-M and poly-MG samples, and a coherence between the estimated sulfation degrees and the relative efficacy of the samples was observed. This was most illustratively shown with the relative efficacy of the 2 % S-MG (DS = 0.08) and the 5 % S-MG (DS = 1.08) samples, where the latter sample was the more effective in all performed protein binding experiments. It is, as mentioned, reasonable to believe that the high solubility of the poly-MG alginates resulted in a more homogenous sulfation pattern, which may be equally significant as the sulfation degree. The conformation difference between poly-M and poly-MG also provides different orientations of the attached sulfate groups, which may also affect the binding affinities of the alginates. The molecular weight discrepancy between the poly-M and poly-MG samples complicated assessment of the impact of flexibility for the protein binding abilities of the different sulfated alginates. The longer poly-M chains were expected to exhibit more available binding sites, while the

lower molecular weight of the poly-MG chains resulted in a higher sample molarity at the given concentrations. Future studies would require a standardization of the sulfation conditions as well as the molecular weight of the samples in order to assess the relative sample effectiveness with confidence. Nonetheless, sulfation of the alginates resulted in a protein binding ability comparable to that of heparin, with a profound increase in effectivity compared to the relatively inert unmodified poly-M and poly-M alginates.

The dose-response of OPG binding was not studied; instead a single concentration (3 µg/ml) of heparin or sulfated alginates was chosen to emphasize the effect of sulfating the alginates in comparison to unmodified alginates. The heparin and sulfated alginate treatments showed a similar degree of OPG release from the cell surface due to the relatively high sample concentrations, which were at the upper limit of the effective dose range obtained in the previous HGF experiment. In contrast with the HGF binding experiments, the heparin and the most potent sulfated alginates were not able to reach the lower MFI value of the positive control, possibly caused by an overall lower affinity of the polysaccharides to OPG. Similarly as in the HGF-binding assay, the unmodified poly-M and poly-MG samples showed no apparent binding to OPG, as they at the same dose failed to release a measurable amount of protein from the cell surface. These results clearly showed an increase in the OPG protein binding ability of the alginates as a result of sulfation.

When studying the induced increase in plasma coagulation time, a drastic difference in the effective dose window was seen when comparing heparin and sulfated alginates. This was an expected result, considering that the coagulation inhibition in the current assay was primarily induced by heparin/antithrombin III-catalyzed inactivation of the supplemented factor Xa. The AT-heparin interaction is highly specific and based on the pentasaccharide sequence illustrated in Figure 5, which is not found in the sulfated alginates. It was, however, observed that the sulfated alginates caused an increase in coagulation time when compared with the unmodified poly-M and poly-MG alginates. The attached sulfate groups add to the inherent negative charge of the alginate, facilitating stronger electrostatic interactions either with factor Xa directly, or indirectly through other plasma components. It is not certain whether the interaction has an allosteric effect on the activity of the bound protein or if the sulfated alginates inhibit the factors by sequestering them from their targets in the coagulation pathway. Also, a relative efficacy difference was

observed coherent with the estimated sulfation degrees, although the 5 % S-MG showed a profoundly greater effect than any of the other samples. As discussed above, it was difficult to assess the relative efficacy of the samples based on sulfation degree estimations alone, since there was a disparity in molecular weight between the poly-M and poly-MG samples, and as the acidic sulfation reaction was likely to have affected the sulfation pattern to a varying extent. The observed high effect of 5 % S-MG may be credited to its high estimated DS, higher flexibility and sample molarity, as well as a substitution pattern expected to be dissimilar to that of the sulfated poly-M alginates. It is still reasonable to assume that the flexibility of the alginate is significant for the properties studied. The conformational flexibility of heparin credited to the iduronic acid monomer has been postulated to confer important binding properties to the heparin and heparan sulfate (Rees, Morris et al. 1985). Similarly, a high conformational flexibility may enable alginates to adapt more easily to irregular surfaces and utilize additional binding sites on proteins.

Upon repeating the experiment, an irregularity in the recorded coagulation times at high treatment concentrations was seen, although the observed relative efficacy of the samples remained the same, showing 5 % S-MG as the most effective treatment after heparin. The aberrations were assumed to be a result of using different blood plasma donors for the two experiments, but could potentially by caused by a decreased sustainability of the plasma, treatment or other assay components over time. As the main aberrations were observed at higher concentrations, it should also be considered that the reliability of the assay may decrease at high treatment concentrations, which to confirm would have required additional experiments covering a larger dose range.

# 5 Prospective Research

The sulfated alginates derived in the present study showed a relatively low efficacy in terms of protein binding and particularly in prolongation of the coagulation time compared to heparin. It was, however, shown that sulfation drastically improved the assayed properties of the alginates compared to the unmodified poly-M and poly-MG alginates. Creating an alginate-derived heparin analog with equally prominent anticoagulating properties may prove difficult due to the absence of a specific AT-activating sequence. Still, it has been shown that it is possible to obtain the effects of heparin caused by non-specific interactions, which may be further optimized by increasing the sulfation degree and flexibility. It is possible and may be desirable to achieve a more moderate therapeutic effect, preferably also with less adverse effects, through the use of a sulfated alginate with a regularity in molecular weight, sequence and modification pattern.

There are improvements to be made with the prospect of more thorough characterization of the sulfated alginates through $^{13}C$ NMR analysis. Producing and analyzing a sulfated poly-G alginate would be essential for unambiguous assignation of the sulfated poly-MG spectrum, as the polyalternating alginate still remains a prime candidate for developing a functional heparin analog due to the high solubility and conformational flexibility. It is also desirable to increase the quantitative reliability of the $^{13}C$ NMR analysis, either through increasing the $^{13}C$ abundance through incorporation of the isotope during the alginate synthesis, or by increasing the recycle delay in the NMR experiments to ensure full relaxation. These efforts would also be likely to increase the resolution of the spectra and reduce noise, contributing to the processes of correct peak assignation and signal integration.

Milder sulfation techniques would contribute to a more predicted response with respect to reaction conditions and the resulting sulfation degrees, and may provide a higher DS than achieved in the current study. It is also likely to reduce the formation of reaction by-products, making the purifying process less complicated and time-consuming. A more homogenous sulfation pattern would also be expected by reducing the acidity of the reaction and thus precipitation of the alginate, which would be a necessity when studying the relative impact of sulfation degree and flexibility on the efficacy of the sulfated

alginates. Of particular interest is the sulfation technique described by Fan and coworkers, involving the use of the sulfating agent ($N(SO_3Na)_3$) (Fan, Jiang et al. 2011), which has also proven applicable for sulfation of other polysaccharides. The flexibility of the poly-MG alginate can be further increased prior to sulfation through periodate oxidation, resulting in greater solubility and potentially leading to an increased sulfation degree and a stronger biological effect.

In further assessment of anticoagulating properties it would be desirable to study the activity of the sulfated alginates using several different assays and determe the response over an increased dose range, as some aberrations were observed at high concentrations in the present study. It is also of interest to eventually create shorter sulfated alginate chains and oligomers to assess maximal sulfation degree and study chain length dependency in various interactions. Furthermore, the sulfated alginates may be incorporated into alginate gel systems to facilitate beneficial interactions, for instance with encapsulated cells or in tissue engineering systems using alginate gel matrices.

# 6 Concluding Remarks

Poly-M and poly-MG alginates were successfully sulfated using the sulfating agent chlorosulfonic acid in formamide. Covalently attached sulfate groups to the alginate were detected using FTIR spectroscopy and confirmed through elemental analysis and $^{13}C$ NMR spectroscopy. The more flexible poly-MG alginates showed a higher solubility in formamide compared to poly-M, resulting in higher sulfation degrees at lower chlorosulfonic acid concentrations, as estimated by elemental analysis. The structures of the sulfated alginates were studied using NMR, and a characterization of the novel signals was proposed for the sulfated poly-M samples. A secondary estimation of the sulfation degrees was also elaborated through integration of the $^{13}C$ spectra. Analysis with SEC-MALLS showed no pronounced degradation of the alginate as a result of sulfation. A vast improvement was seen in the ability of sulfated alginates to bind hepatocyte growth factor and osteoprotegerin when compared with unmodified poly-M and poly-MG alginates. Sulfation of the alginates also resulted in measurable prolongation of plasma coagulation time, although a large increase in dose was required to achieve this effect, compared with heparin. Of the tested sulfated alginates, the poly-MG alginate with the highest estimated sulfation degree exhibited the highest degree of protein binding and the largest increase in plasma coagulation time.

The results showed that alginates can be modified to exhibit biological properties analogous to heparin through chemical sulfation, and that the analog can be structurally characterized using the techniques described in this thesis. It was also proposed that the methods could be further optimized, primarily through standardization of the sulfation conditions, to amplify the biological effects achieved and to obtain more confident qualitative and quantitative data for the structural characterization of the analog.

# References


Alshamkhani, A. and R. Duncan (1995). "Radioiodination of Alginate Via Covalently-Bound Tyrosinamide Allows Monitoring of Its Fate in-Vivo." Journal of Bioactive and Compatible Polymers **10**(1): 4-13.

Augst, A. D., H. J. Kong, et al. (2006). "Alginate hydrogels as biomaterials." Macromolecular Bioscience **6**(8): 623-633.

Balakrishnan, B., M. Mohanty, et al. (2005). "Evaluation of an in situ forming hydrogel wound dressing based on oxidized alginate and gelatin." Biomaterials **26**(32): 6335-6342.

Bar-Yosef, S., H. B. Cozart, et al. (2007). "Preoperative low molecular weight heparin reduces heparin responsiveness during cardiac surgery." Canadian Journal of Anaesthesia-Journal Canadien D Anesthesie **54**(2): 107-113.

Bhaskar, U., E. Sterner, et al. (2012). "Engineering of routes to heparin and related polysaccharides." Appl Microbiol Biotechnol **93**(1): 1-16.

Bouhadir, K. H., K. Y. Lee, et al. (2001). "Degradation of partially oxidized alginate and its potential application for tissue engineering." Biotechnol Prog **17**(5): 945-950.

Breger, J. C., D. B. Lyle, et al. (2009). "Defining Critical Inflammatory Parameters for Endotoxin Impurity in Manufactured Alginate Microcapsules." Journal of Biomedical Materials Research Part B-Applied Biomaterials **91B**(2): 755-765.

Bubb, W. A. (2003). "NMR spectroscopy in the study of carbohydrates: Characterizing the structural complexity." Concepts in Magnetic Resonance Part A **19A**(1): 1-19.

Børset, M., H. Hjorth Hansen, et al. (1996). "Hepatocyte growth factor and its receptor c-met in multiple myeloma." Blood **88**(10): 3998-4004.

Castelli, R., F. Porro, et al. (2004). "The heparins and cancer: review of clinical trials and biological properties." Vascular Medicine **9**(3): 205-213.

Casu, B., P. Oreste, et al. (1981). "The Structure of Heparin Oligosaccharide Fragments with High Anti-(Factor-Xa) Activity Containing the Minimal Antithrombin-Iii-Binding Sequence - Chemical and C-13 Nmr-Studies." Biochemical Journal **197**(3): 599-609.

Cathell, M. D., J. C. Szewczyk, et al. (2010). "Organic Modification of the Polysaccharide Alginate." Mini-Reviews in Organic Chemistry **7**(1): 61-67.

Chen, J. H. and J. Liu (2005). "Characterization of the structure of antithrombin-binding heparan sulfate generated by heparan sulfate 3-O-sulfotransferase 5." Biochimica Et Biophysica Acta-General Subjects **1725**(2): 190-200.

Chen, Y. P., T. Maguire, et al. (1997). "Dengue virus infectivity depends on envelope protein binding to target cell heparan sulfate." Nature Medicine **3**(8): 866-871.

Chong, B. H. (2003). "Heparin-induced thrombocytopenia." J Thromb Haemost **1**(7): 1471-1478.

Conrad, H. E. (1998). Heparin-binding proteins. San Diego, Academic Press.

De Candia, E., R. De Cristofaro, et al. (1999). "Thrombin induced platelet activation is inhibited by high and low molecular weight heparin." Thrombosis and Haemostasis: 822-822.

Donati, I., A. Vetere, et al. (2003). "Galactose-substituted alginate: Preliminary characterization and study of gelling properties." Biomacromolecules **4**(3): 624-631.

Doran, P. M. (1995). Bioprocess engineering principles / Pauline M. Doran. London, Academic Press.

Doucleff, M., M. Hatcher-Skeers, et al. (2011). Pocket Guide to Biomolecular NMR. New York, Springer.

Draget, K. I., G. Skjåk-Bræk, et al. (1997). "Alginate based new materials." Int J Biol Macromol **21**(1-2): 47-55.

Ernst, S., G. Venkataraman, et al. (1998). "Pyranose ring flexibility. Mapping of physical data for iduronate in continuous conformational space." Journal of the American Chemical Society **120**(9): 2099-2107.

Ertesvåg, H., H. K. Høidal, et al. (1999). "Mannuronan C-5-epimerases and their application for in vitro and in vivo design of new alginates useful in biotechnology." Metab Eng **1**(3): 262-269.

Fan, L. H., S. Gao, et al. (2012). "Synthesis and anticoagulant activity of pectin sulfates." Journal of Applied Polymer Science **124**(3): 2171-2178.

Fan, L. H., L. Jiang, et al. (2011). "Synthesis and anticoagulant activity of sodium alginate sulfates." Carbohydrate Polymers **83**(4): 1797-1803.

Fan, L. H., P. Wu, et al. (2012). "Synthesis and anticoagulant activity of the quaternary ammonium chitosan sulfates." Int J Biol Macromol **50**(1): 31-37.

Forsten, K. E., M. Fannon, et al. (2000). "Potential mechanisms for the regulation of growth factor binding by heparin." Journal of Theoretical Biology **205**(2): 215-230.

Franchini, M. (2005). "Heparin-induced thrombocytopenia: an update." Thromb J **3**: 14.

Freeman, I., A. Kedem, et al. (2008). "The effect of sulfation of alginate hydrogels on the specific binding and controlled release of heparin-binding proteins." Biomaterials **29**(22): 3260-3268.

Gao, C. J., B. Boylan, et al. (2011). "Heparin promotes platelet responsiveness by potentiating alpha IIb beta 3-mediated outside-in signaling." Blood **117**(18): 4946-4952.

Gimmestad, M., H. Sletta, et al. (2003). "The Pseudomonas fluorescens AlgG protein, but not its mannuronan C-5-epimerase activity, is needed for alginate polymer formation." Journal of Bacteriology **185**(12): 3515-3523.

Glicksman, M. (1987). "Utilization of Seaweed Hydrocolloids in the Food-Industry." Hydrobiologia **151**: 31-47.

Gomez, C. G., M. Rinaudo, et al. (2007). "Oxidation of sodium alginate and characterization of the oxidized derivatives." Carbohydrate Polymers **67**(3): 296-304.

Grasdalen, H., B. Larsen, et al. (1981). "C-13-Nmr Studies of Monomeric Composition and Sequence in Alginate." Carbohydrate Research **89**(2): 179-191.

Greer, I. and B. J. Hunt (2005). "Low molecular weight heparin in pregnancy: current issues." Br J Haematol **128**(5): 593-601.

Habuchi, O. (2000). "Diversity and functions of glycosaminoglycan sulfotransferases." Biochimica Et Biophysica Acta-General Subjects **1474**(2): 115-127.

Hirsh, J. (1998). "Low-molecular-weight heparin : A review of the results of recent studies of the treatment of venous thromboembolism and unstable angina." Circulation **98**(15): 1575-1582.

Hirsh, J., S. S. Anand, et al. (2001). "Guide to anticoagulant therapy: Heparin : a statement for healthcare professionals from the American Heart Association." Circulation **103**(24): 2994-3018.

Hirsh, J., S. S. Anand, et al. (2001). "Mechanism of action and pharmacology of unfractionated heparin." Arteriosclerosis Thrombosis and Vascular Biology **21**(7): 1094-1096.

Hirsh, J. and R. Raschke (2004). "Heparin and low-molecular-weight heparin - The Seventh ACCP Conference on Antithrombotic and Thrombolytic Therapy." Chest **126**(3): 188s-203s.

Hu, X. K., X. L. Jiang, et al. (2004). "Antitumour activities of alginate-derived oligosaccharides and their sulphated substitution derivatives." European Journal of Phycology **39**(1): 67-71.

Huang, R. H., Y. M. Du, et al. (2003). "Preparation and in vitro anticoagulant activities of alginate sulfate and its quaterized derivatives." Carbohydrate Polymers **52**(1): 19-24.

Huntington, J. A. and T. P. Baglin (2003). "Targeting thrombin - rational drug design from natural mechanisms." Trends in Pharmacological Sciences **24**(11): 589-595.

Ikeda, A., A. Takemura, et al. (2000). "Preparation of low-molecular weight alginic acid by acid hydrolysis." Carbohydrate Polymers **42**(4): 421-425.

Irie, A., M. Takami, et al. (2007). "Heparin enhances osteoclastic bone resorption by inhibiting osteoprotegerin activity." Bone **41**(2): 165-174.

Jacobsson, K. G., J. Riesenfeld, et al. (1985). "Biosynthesis of Heparin - Effects of Normal-Butyrate on Cultured Mast-Cells." Journal of Biological Chemistry **260**(22): 2154-2159.

Jain, S., M. J. Franklin, et al. (2003). "The dual roles of AlgG in C-5-epimerization and secretion of alginate polymers in Pseudomonas aeruginosa." Molecular Microbiology **47**(4): 1123-1133.

Jones, C. J., S. Beni, et al. (2011). "Heparin characterization: challenges and solutions." Annu Rev Anal Chem (Palo Alto Calif) **4**: 439-465.

Kelton, J. G. (2002). "Heparin-induced thrombocytopenia: an overview." Blood Rev **16**(1): 77-80.

Khorana, A. A., A. Sahni, et al. (2003). "Heparin inhibition of endothelial cell proliferation and organization is dependent on molecular weight." Arteriosclerosis Thrombosis and Vascular Biology **23**(11): 2110-2115.

Klock, G., A. Pfeffermann, et al. (1997). "Biocompatibility of mannuronic acid-rich alginates." Biomaterials **18**(10): 707-713.

Kong, H. J., M. K. Smith, et al. (2003). "Designing alginate hydrogels to maintain viability of immobilized cells." Biomaterials **24**(22): 4023-4029.

Kragh, M., L. Binderup, et al. (2005). "Non-anti-coagulant heparin inhibits metastasis but not primary tumor growth." Oncology Reports **14**(1): 99-104.

Kusche, M. and U. Lindahl (1990). "Biosynthesis of Heparin - O-Sulfation of D-Glucuronic Acid Units." Journal of Biological Chemistry **265**(26): 15403-15409.

Lam, L. H., J. E. Silbert, et al. (1976). "The separation of active and inactive forms of heparin." Biochem Biophys Res Commun **69**(2): 570-577.

Lambert, J. B. (1998). Organic structural spectroscopy. Upper Saddle River, N.J., Prentice Hall.

Lee, K. Y. and D. J. Mooney (2012). "Alginate: properties and biomedical applications." Prog Polym Sci **37**(1): 106-126.

Lefkou, E., M. Khamashta, et al. (2010). "Review: Low-molecular-weight heparin-induced osteoporosis and osteoporotic fractures: a myth or an existing entity?" Lupus **19**(1): 3-12.

Lehninger, A. L., D. L. Nelson, et al. (2008). Lehninger principles of biochemistry. New York, W.H. Freeman.

Li, B., J. Suwan, et al. (2009). "Oversulfated chondroitin sulfate interaction with heparin-binding proteins: new insights into adverse reactions from contaminated heparins." Biochem Pharmacol **78**(3): 292-300.

Lormeau, J. C., J. P. Herault, et al. (1996). "Antithrombin-mediated inhibition of factor VIIa-tissue factor complex by the synthetic pentasaccharide representing the heparin binding site to antithrombin." Thrombosis and Haemostasis **76**(1): 5-8.

Marciniak, E. and J. P. Gockerman (1977). "Heparin-Induced Decrease in Circulating Antithrombin-3." Lancet **2**(8038): 581-584.

Mendes, S. F., O. dos Santos, Jr., et al. (2009). "Sulfonation and anticoagulant activity of botryosphaeran from Botryosphaeria rhodina MAMB-05 grown on fructose." Int J Biol Macromol **45**(3): 305-309.

Nahmias, A. J. and S. Kibrick (1964). "Inhibitory Effect of Heparin on Herpes Simplex Virus." Journal of Bacteriology **87**(5): 1060-&.

O'Reilly, M. S., S. Pirie-Shepherd, et al. (1999). "Antiangiogenic activity of the cleaved conformation of the serpin antithrombin." Science **285**(5435): 1926-1928.

Okeeffe, D. J., T. P. Baglin, et al. (2004). "The heparin binding properties of heparin cofactor II suggest an antithrombin-like activation mechanism." Blood **104**(11): 477a-477a.

Orgueira, H. A., A. Bartolozzi, et al. (2003). "Modular synthesis of heparin oligosaccharides." Chemistry-a European Journal **9**(1): 140-169.

Parra, A., N. Veraldi, et al. (2012). "Heparin-like heparan sulfate from rabbit cartilage." Glycobiology **22**(2): 248-257.

Pawar, S. N. and K. J. Edgar (2011). "Chemical modification of alginates in organic solvent systems." Biomacromolecules **12**(11): 4095-4103.

Pawar, S. N. and K. J. Edgar (2012). "Alginate derivatization: A review of chemistry, properties and applications." Biomaterials **33**(11): 3279-3305.

Petitou, M. and C. A. A. van Boeckel (2004). "A synthetic antithrombin III binding pentasaccharide is now a drug! What comes next?" Angewandte Chemie-International Edition **43**(24): 3118-3133.

Podzimek, S. (2011). Light scattering, size exclusion chromatography, and asymmetric flow field flow fractionation : powerful tools for the characterization of polymers, proteins and nanoparticles. Hoboken, N.J., Wiley.

Preissner, K. T. and G. Muller-Berghaus (1987). "Neutralization and binding of heparin by S protein/vitronectin in the inhibition of factor Xa by antithrombin III. Involvement of an inducible heparin-binding domain of S protein/vitronectin." J Biol Chem **262**(25): 12247-12253.

Quinn, K. J., J. M. Courtney, et al. (1985). "Principles of burn dressings." Biomaterials **6**(6): 369-377.

Rastello De Boisseson, M., M. Leonard, et al. (2004). "Physical alginate hydrogels based on hydrophobic or dual hydrophobic/ionic interactions: bead formation, structure, and stability." J Colloid Interface Sci **273**(1): 131-139.

Rees, D. A., E. R. Morris, et al. (1985). "Controversial Glycosaminoglycan Conformations." Nature **317**(6037): 480-480.

Rehm, B. H. and S. Valla (1997). "Bacterial alginates: biosynthesis and applications." Appl Microbiol Biotechnol **48**(3): 281-288.

Rowley, J. A., G. Madlambayan, et al. (1999). "Alginate hydrogels as synthetic extracellular matrix materials." Biomaterials **20**(1): 45-53.

Sabbagh, A. H., G. K. T. Chung, et al. (1984). "Fresh-Frozen Plasma - a Solution to Heparin Resistance during Cardiopulmonary Bypass." Annals of Thoracic Surgery **37**(6): 466-468.

Sakugawa, K., A. Ikeda, et al. (2004). "Simplified method for estimation of composition of alginates by FTIR." Journal of Applied Polymer Science **93**(3): 1372-1377.

Salzman, E. W., R. D. Rosenberg, et al. (1980). "Effect of Heparin and Heparin Fractions on Platelet-Aggregation." Journal of Clinical Investigation **65**(1): 64-73.

Sasisekharan, R. and G. Venkataraman (2000). "Heparin and heparan sulfate: biosynthesis, structure and function." Curr Opin Chem Biol **4**(6): 626-631.

Scott, J. E. and R. J. Harbinson (1969). "Periodate Oxidation of Acid Polysaccharides .2. Rates of Oxidation of Uronic Acids in Polyuronides and Acid Mucopolysaccharides." Histochemie **19**(2): 155-&.

Seidel, C., H. Hjorth-Hansen, et al. (1999). "Hepatocyte growth factor in serum after injection of unfractionated and low molecular weight heparin in healthy individuals." British Journal of Haematology **105**(3): 641-647.

Shaughnessy, S. G., E. Young, et al. (1995). "The effects of low molecular weight and standard heparin on calcium loss from fetal rat calvaria." Blood **86**(4): 1368-1373.

Shukla, D., J. Liu, et al. (1999). "A novel role for 3-O-sulfated heparan sulfate in herpes simplex virus 1 entry." Glycobiology **9**(10): 1142-1142.

Simsek-Ege, F. A., G. M. Bond, et al. (2003). "Polyelectrolye complex formation between alginate and chitosan as a function of pH." Journal of Applied Polymer Science **88**(2): 346-351.

Skjåk-Bræk, G., H. Grasdalen, et al. (1986). "Monomer Sequence and Acetylation Pattern in Some Bacterial Alginates." Carbohydrate Research **154**: 239-250.

Smidsrød, O. (1973). "Relative Extension of Alginates Having Different Chemical Composition." Carbohydrate Research **27**(1): 107-118.

Smidsrød, O. and G. Skjåk-Bræk (1990). "Alginate as immobilization matrix for cells." Trends Biotechnol **8**(3): 71-78.

Stuart, B. (2004). Infrared spectroscopy : fundamentals and applications. Chichester, England ; Hoboken, NJ, J. Wiley.

Triplett, D. A. (2000). "Coagulation and bleeding disorders: Review and update." Clinical Chemistry **46**(8B): 1260-1269.

Valla, S., J. P. Li, et al. (2001). "Hexuronyl C5-epimerases in alginate and glycosaminoglycan biosynthesis." Biochimie **83**(8): 819-830.

van Doormaal, F. F., M. Di Nisio, et al. (2011). "Randomized Trial of the Effect of the Low Molecular Weight Heparin Nadroparin on Survival in Patients With Cancer." Journal of Clinical Oncology **29**(15): 2071-2076.

Warkentin, T. E., M. N. Levine, et al. (1995). "Heparin-Induced Thrombocytopenia in Patients Treated with Low-Molecular-Weight Heparin or Unfractionated Heparin." New England Journal of Medicine **332**(20): 1330-1335.

Weitz, J. I., E. Young, et al. (1999). "Vasoflux, a new anticoagulant with a novel mechanism of action." Circulation **99**(5): 682-689.

Wiebe, E. M., A. R. Stafford, et al. (2003). "Mechanism of catalysis of inhibition of factor IXa by antithrombin in the presence of heparin or pentasaccharide." Journal of Biological Chemistry **278**(37): 35767-35774.

Yu, H. and X. Chen (2007). "Carbohydrate post-glycosylational modifications." Org Biomol Chem **5**(6): 865-872.

Zhu, Q. W., L. T. Yang, et al. (2007). "Preparation of flusilazole sodium alginate microcapsule by duplicate emulsification and studies on sustained release." Chemical Journal on Internet **9**(5): 24.

# Appendices

## A. SEC-MALLS Output Data

The molecular weight averages and distributions of the unmodified and sulfated alginate samples were studied using SEC-MALLS. The data for the poly-M and poly-MG samples studied are listed in Table A 1 and Table A 2, and the distributions are illustrated in the chromatography charts shown in Figure A 1 and Figure A 2, respectively.

Symbols and abbreviations:

$M_n$ = Molecular number average

$M_w$ = Molecular weight average

Rz = Radius of gyration from the angle dependence of light scattering

dn/dc = Refractive index

**Table A 1: SEC-MALLS data for unmodified (Poly-M) and sulfated polymannuronic acid (S-M) samples.**

| | $M_n$ (kDa) | $M_w$ (kDa) | Polydispersity (Mw/Mn) | Rz (nm) | Injected mass (µg) | Calculated mass (µg) | dn/dc (ml/g) | Peak limits (min) |
|---|---|---|---|---|---|---|---|---|
| **Poly-M** | 23.8 | 32.1 | 1.35 | 27.7 | 75 | 5.86E+01 | 0.15 | 19.82 - 23.61 |
| **2 % S-M** | 23.0 | 30.6 | 1.33 | 21.5 | 150 | 6.31E+01 | 0.15 | 19.98 - 24.41 |
| **5 % S-M** | 22.1 | 31.4 | 1.43 | 18.7 | 150 | 5.57E+01 | 0.15 | 20.09 - 25.16 |
| **10 % S-M** | 24.2 | 32.6 | 1.35 | 18.5 | 150 | 6.11E+01 | 0.15 | 20.07 - 24.45 |
| **Average** | 23.3 | 31.7 | 1.36 | 21.6 | 131.3 | 5.96E+01 | 0.15 | |
| **Standard deviation** | 1.4 | 1.3 | 0.05 | 4.8 | 64.9 | 4.80E+00 | 0 | |
| **% Standard deviation** | 6.2 | 4.1 | 3.56 | 22.4 | 49.5 | 8.05E+00 | 0 | |
| **Minimum** | 22.1 | 30.6 | 1.33 | 18.5 | 75 | 5.57E+01 | 0.15 | |
| **Maximum** | 24.2 | 32.6 | 1.43 | 27.7 | 150 | 6.31E+01 | 0.15 | |

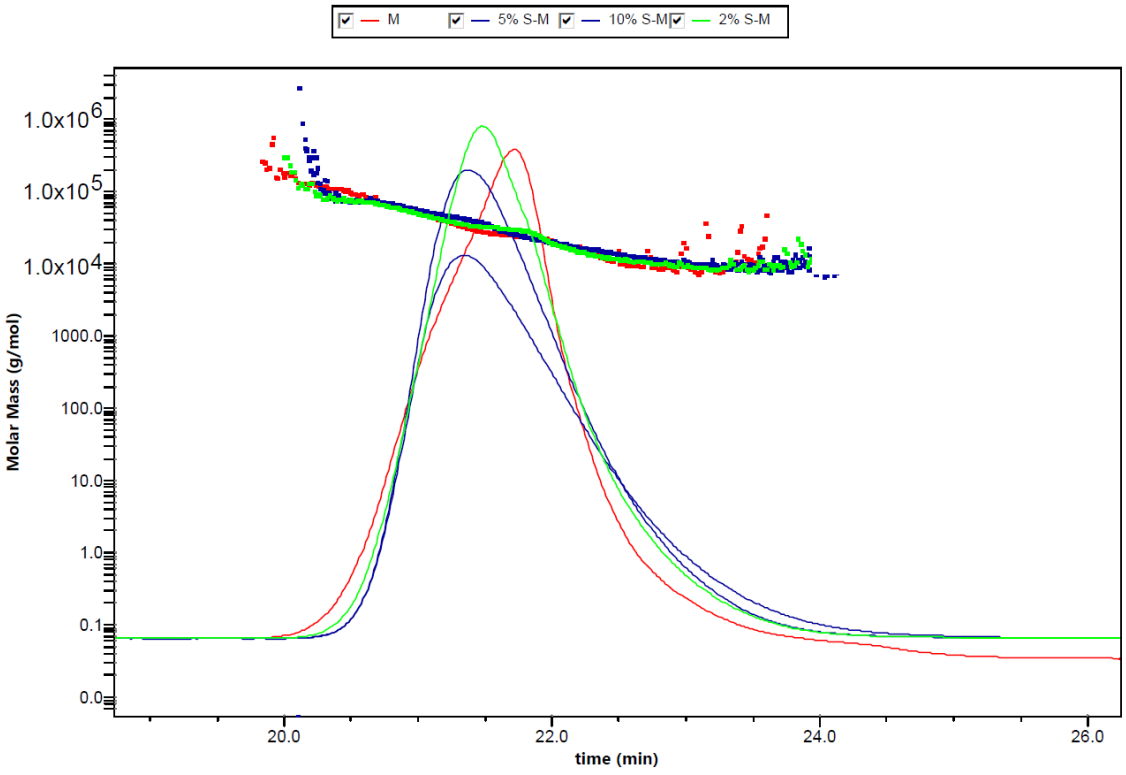


**Figure A 1: Chromatography chart from SEC-MALLS analysis of unmodified (M) and sulfated (S-M) polymannuronic acid samples. A refractive index (dn/dc) value of 0.15 was used for all samples.**

**Table A 2: SEC-MALLS data for unmodified (Poly-MG) and sulfated (S-MG) polyalternating alginate samples.**

| | Mn (kDa) | Mw (kDa) | Polydispersity (Mw/Mn) | Rz (nm) | Injected mass (µg) | Calculated mass (µg) | dn/dc (ml/g) | Peak limits (min) |
|---|---|---|---|---|---|---|---|---|
| **Poly-MG** | 11.8 | 14.3 | 1.21 | 12.5 | 150 | 1.21E+02 | 0.15 | 20.44 - 24.63 |
| **1 % S-MG** | 12.1 | 17.0 | 1.41 | 15.1 | 150 | 6.23E+01 | 0.15 | 20.23 - 26.18 |
| **2 % S-MG** | 12.8 | 18.4 | 1.43 | 15.6 | 150 | 6.40E+01 | 0.15 | 20.19 - 25.98 |
| **5 % S-MG** | 15.8 | 22.9 | 1.45 | 17.0 | 150 | 4.99E+01 | 0.15 | 20.38 - 26.08 |
| **Average** | 13.2 | 18.2 | 1.37 | 15.1 | 150 | 7.42E+01 | 0.15 | |
| **Standard deviation** | 2.1 | 5.0 | 0.19 | 3.0 | 0 | 3.66E+01 | 0 | |
| **% Standard deviation** | 15.8 | 27.3 | 13.81 | 20 | 0 | 4.94E+01 | 0 | |
| **Minimum** | 11.8 | 14.3 | 1.21 | 12.5 | 150 | 4.99E+01 | 0.15 | |
| **Maximum** | 15.8 | 22.9 | 1.45 | 17.0 | 150 | 1.21E+02 | 0.15 | |

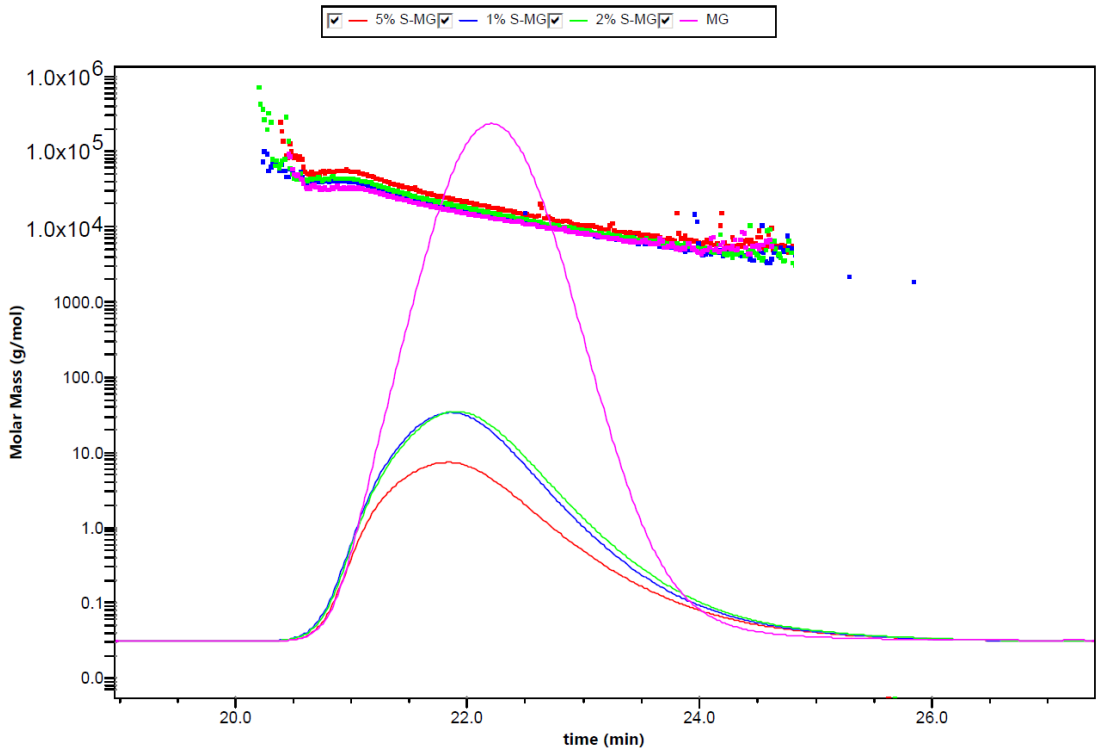


**Figure A 2: Chromatography chart from SEC-MALLS analysis of unmodified (MG) and sulfated (S-MG) polyalternating alginate samples. A refractive index (dn/dc) value of 0.15 was used for all samples.**

## B. Elemental Analysis Data - Calculation of Degrees of Sulfation

The degrees of sulfation (DS) of the sulfated alginates were estimated through measurement of the sulfur contents in the samples using HR-ICP-MS, followed by correlation of the data to a standard curve based on theoretical sulfur content of a sulfated alginate with set DS values. Standard curve values were derived from a mass balance equation including the sulfated alginate monomer as well as associated water molecules and counter-ions.

Calculation example of standard curve values:

The referential degree of sulfation x = 2 was inserted into the mass balance equation 2.1 previously elaborated, and the total monomer mass was calculated as shown below.

$$Mass = C_6O_6H_5 + (x+1)Na^+ + xSO_3^- + H_2O$$

$$= 173.1 \text{ g/mol} + (2+1)23 \text{ g/mol} + (2)80 \text{ g/mol} + 18 \text{ g/mol}$$

$$= 420.1 \text{ g/mol}$$

The sulfur content in percent was found by dividing the molecular weight of the sulfur by the calculated total monomer mass, and is shown in Table B 1 with corresponding DS values from 0 to the theoretical maximum of 2. The sulfur content was graphed as a function of DS, and a second degree function was fitted to the standard curve, shown in Figure B 1.

$$\text{Mass sulfur} = \frac{2 \times 32\ \text{g/mol}}{420.1\ \text{g/mol}} \times 100\ \% = 15.2\ \%$$

**Table B 1: Calculated mass and sulfur content of sulfated alginate monomers for standard curve plot.**

| DS | Mass (g/mol) | %S |
|---|---|---|
| 2 | 420.1 | 15.2 |
| 1.5 | 368.6 | 13.0 |
| 1 | 317.1 | 10.1 |
| 0.5 | 265.6 | 6.0 |
| 0 | 214.1 | 0.0 |

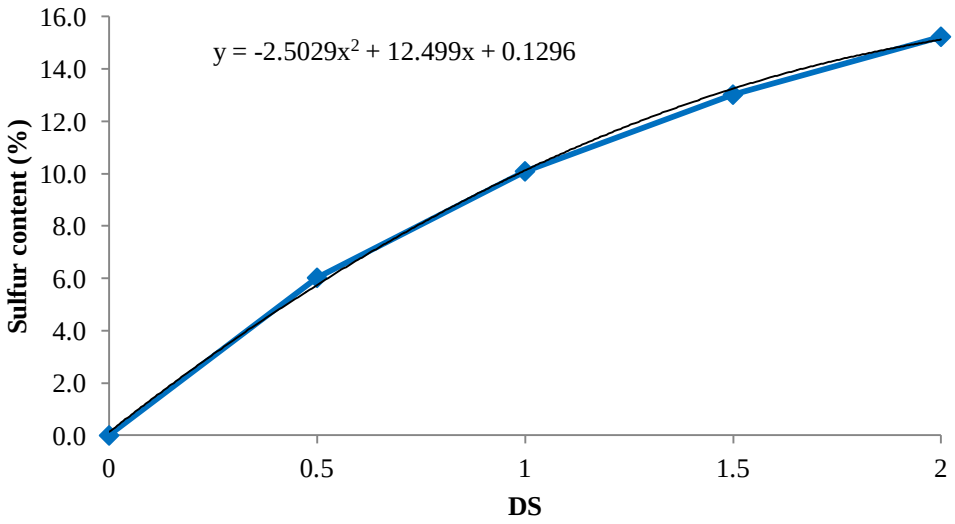


**Figure B 1: Standard curve of theoretical sulfur content (%) in sulfated alginates as a function of degree of sulfation (DS). A second degree function was fitted to the curve with the equation shown in the graph.**

Calculation example of sample DS:

The sulfur content in the 2 % S-M sample was measured at 1.6124 %, which was inserted into the standard curve equation shown in Figure B 1. The calculated value for x corresponded to the estimated degree of sulfation for the sample, giving in the values listed in Table B 2.

$1.6124 = -2.5029x^2 + 12.499x + 0.1296$

$-2.5029x^2 + 12.499x - 1.4828 = 0$

$ax^2 + by + c = 0$

$$x = \frac{-b \pm \sqrt{b^2 - 4ac}}{2a}$$

x = 0.1216

**Table B 2: Calculated degrees of sulfation (DS) in poly-M and poly-MG alginates sulfated using chlorosulfonic acid concentrations of 1 %, 2 %, 5 % and 10 %, based on the sulfur contents of the samples measured through HR-ICP-MS, and the derived standard curve equation shown in Figure B 1.**

| Sample | S (ug/g) | %S | x = DS |
|---|---|---|---|
| **2 % S-M** | 16 124 | 1.6124 | 0.1216 |
| **5 % S-M** | 91 359 | 9.1359 | 0.8732 |
| **10 % S-M** | 82 222 | 8.2222 | 0.7645 |
| **1 % S-MG** | 10 774 | 1.0774 | 0.0770 |
| **2 % S-MG** | 60 921 | 6.0921 | 0.5342 |
| **5 % S-MG** | 106 993 | 10.6993 | 1.0787 |

## C. $^{13}$C NMR Integration Values

The integration values for the poly-M $^{13}$C NMR spectra shown in Figure 12 of the thesis are listed below in Table C 1. Estimations of the degrees of sulfation for the samples were made with respect to signals associated with carbons C1 or C2 and C3.

**Table C 1: $^{13}$C NMR integration value for poly-M alginates sulfated using chlorosulfonic acid concentrations of 2 %, 5 % and 10 %, with estimation of sulfation degrees shown in bold. Samples were dissolved in $D_2O$ and the spectra were recorded at 40 °C on a 600 MHz spectrometer with an inverse gated decoupling scheme, 30° pulse angle and 5 seconds intrascan delay.**

| Sample | $I_{C2}$ | $I_{C3}$ | $I_{C2S}$ | $I_{C3S}$ | $\frac{(I_{C2S}+I_{C3S})}{(I_{C2S}+I_{C3S}+I_{C2}+I_{C3})}$ | $I_{C1}$ | $I_{C1(S+SS)}$ | $\frac{(I_{C1(S+SS)})}{(I_{C1(S+SS)}+I_{C1})}$ |
|---|---|---|---|---|---|---|---|---|
| **2 % S-M** | 2.248 | 1.376 | 0.595 | 0.347 | **0.206** | 1.000 | 0.604 | **0.377** |
| **5 % S-M** | 3.006 | 1.887 | 6.641 | 4.641 | **0.697** | 1.000 | 7.775 | **0.886** |
| **10 % S-M** | 1.979 | 1.323 | 1.671 | 1.792 | **0.512** | 1.000 | 2.194 | **0.687** |

## D. Flow Cytometry Data

Myeloma RPMI cells with bound HGF or OPG were treated with heparin and sulfated alginates, and subsequently labeled with fluorescent antibodies (FITC). Flow cytometry was utilized to measure the fluorescence of the cells, corresponding to the amount of remaining bound proteins. The mean fluorescence intensity (MFI), defined as the mean area of the cell count distribution as a function of fluorescing FITC measured (Figure D 1), was recorded for a selected viable cell population.

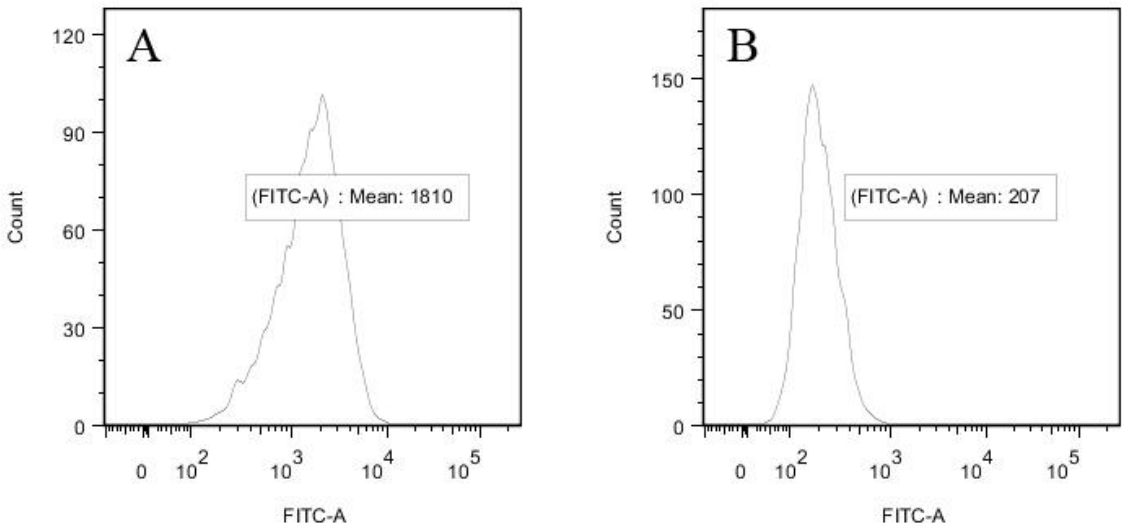


**Figure D 1: Analysis of flow cytometry data using FlowJo. Recording of mean fluorescein isothiocyanate (FITC) area for myeloma RPMI cells with bound HGF. (A) Negative control sample labeled with HGF 2B5 primary antibody and GAM FITC secondary antibody. (B) Isotype control sample labeled with non-HGF binding Mouse $IgG_1$ pure primary antibody and GAM FITC secondary antibody.**

Figure D 2 shows the measured MFI of HGF-stimulated myeloma RPMI cells treated with a single concentration of heparin or the sulfated alginate samples in reference to an untreated negative control and a positive isotype control. The four most potent sulfated alginate samples (5 % S-M, 10 % S-M, 2 % S-MG and 5 % S-MG) were selected for further study.

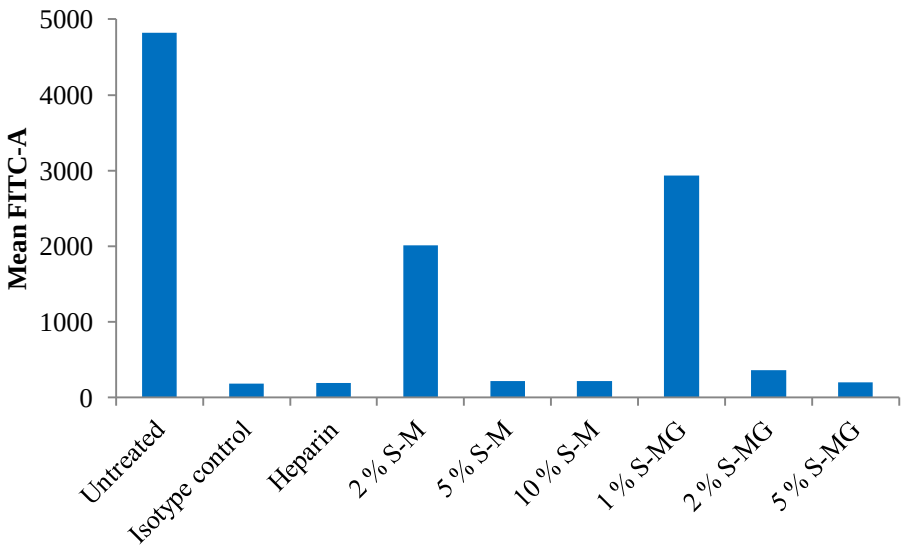


**Figure D 2: Measured mean fluorescence intensity from antibody-labeled HGF proteins bound to myeloma RPMI cell surface, following treatment with 10 µg/ml heparin or poly-M and poly-MG alginates sulfated using 1 %, 2 %, 5 % or 10 % chlorosulfonic acid.**

A dose-response curve was established using heparin and the selected sulfated alginate samples in relation to a positive isotype control, a negative untreated control and unmodified poly-M and poly-MG alginates. The recorded MFI values are listed below in Table D 1 and graphed in Figure D 3 with guidance lines for the proposed dose-response curve.

**Table D 1: Mean fluorescence intensity (MFI) values from flow cytometry of HGF-stimulated cells treated with heparin or poly-M and poly-MG alginates either unmodified or sulfated using chlorosulfonic acid concentrations of 2 %, 5 % or 10 %, and labeled with fluorescein isothiocyanate (FITC) antibody. S-M and S-MG data were collected from separate experiments.**

| | | | MFI | | |
|---|---|---|---|---|---|
| **Concentration (µg/ml)** | **Heparin** | **5 % S-M** | **10 % S-M** | **2 % S-MG** | **5 % S-MG** |
| **10** | 224 | 219 | 216 | 210 | 205 |
| **3** | 204 | 243 | 239 | 292 | 213 |
| **1** | 223 | 351 | 440 | 697 | 258 |
| **0.3** | 365 | 717 | 790 | 1515 | 568 |
| **0.1** | 836 | 1472 | 1740 | 1999 | 1500 |
| **0.01** | 1773 | 1927 | 1827 | 1987 | 2116 |
| **0.001** | 1908 | 1932 | 1476 | 2013 | 1654 |
| | | **Isotype Control** | **Untreated** | **Poly-M (10 µg/ml)** | **Poly-MG (10 µg/ml)** |
| | | 207 | 1798 | 1933 | 1765 |

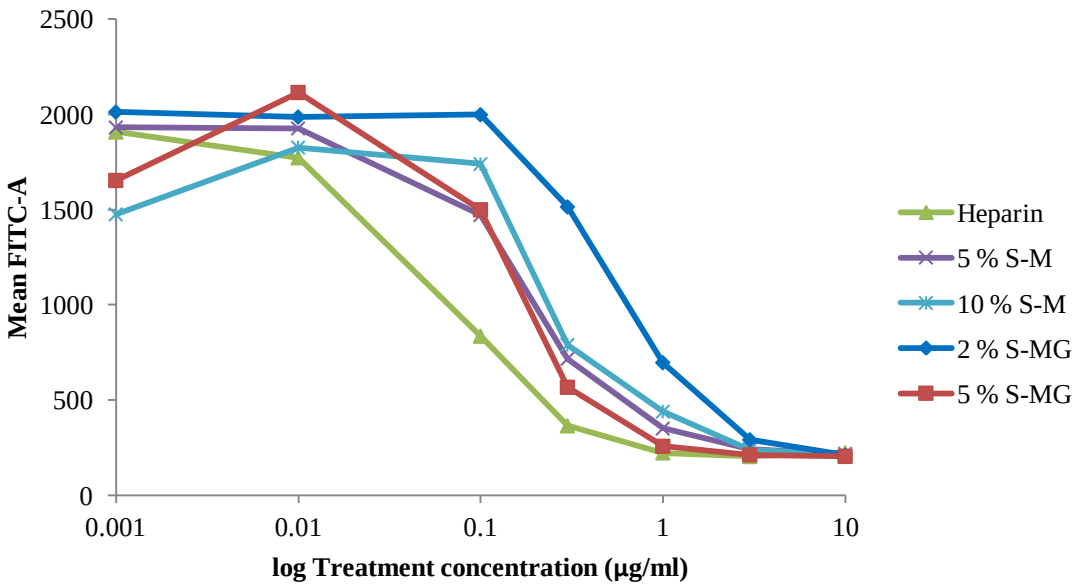


**Figure D 3: Measured mean fluorescent intensity (MFI) from FITC Ab-labeled HGF proteins bound to myeloma RPMI cell surface, following treatment with heparin or poly-M and poly-MG alginates sulfated using 2 %, 5 % or 10 % chlorosulfonic acid. as a function of treatment concentration. S-M and S-MG data were collected from separate experiments.**

The percentage of cell-bound HGF was estimated by dividing the MFI values of the heparin or sulfated alginate samples (Table D 1) by the value of the untreated negative control set to 100 %, and is shown below in Table D 2.

**Table D 2: Calculated percentage of cell-bound HGF following treatment with heparin or sulfated alginates. Mean fluorescence intensities were recorded by flow cytometry and converted to % cell-bound OPG in reference to the untreated control sample. S-M and S-MG data were collected from separate experiments.**

| | Cell-bound HGF (%) | | | | |
|---|---|---|---|---|---|
| **Concentration (µg/ml)** | **Heparin** | **5 % S-M** | **10 % S-M** | **2 % S-MG** | **5 % S-MG** |
| **10** | 12.5 | 12.2 | 12.0 | 11.7 | 11.4 |
| **3** | 11.3 | 13.5 | 13.3 | 16.2 | 11.8 |
| **1** | 12.4 | 19.5 | 24.5 | 38.8 | 14.3 |
| **0.3** | 20.3 | 39.9 | 43.9 | 84.3 | 31.6 |
| **0.1** | 46.5 | 81.9 | 96.8 | 111.2 | 83.4 |
| **0.01** | 98.6 | 107.2 | 101.6 | 110.5 | 117.7 |
| **0.001** | 106.1 | 107.5 | 82.1 | 112.0 | 92.0 |
| **0** | 100.0 | 100.0 | 100.0 | 100.0 | 100.0 |
| | **Untreated** | | **Poly-M (10 µg/ml)** | | **Poly-MG (10 µg/ml)** |
| | 100 | | 107.5 | | 98.9 |

In a separate experiment, myeloma RPMI cells were stimulated with the protein osteoprotegerin (OPG) before treating with a single concentration (3 µg/ml) of heparin or unmodified and sulfated alginates. The cell-bound protein was subsequently labeled with a primary OPG antibody and a secondary fluorescent (FITC) antibodies as previously described, and the fluorescence was measured using flow cytometry. MFI values were converted to cell bound HGF (%) in reference to the untreated negative control set to 100 %, with values listed in Table D 3.

**Table D 3: Mean fluorescence intensity (MFI) values from flow cytometry of osteoprotegerin (OPG)-stimulated cells treated with 3 µg/ml heparin or poly-M and poly-MG alginates either unmodified or sulfated using chlorosulfonic acid concentrations of 2 %, 5 % or 10 %, and labeled with fluorescein isothiocyanate (FITC) antibody. MFI values were converted to cell-bound OPG in reference to the untreated control sample set to 100 % cell-bound OPG.**

| Control samples | MFI | Cell-bound OPG (%) |
|---|---|---|
| Untreated | 920 | 100.0 |
| Isotype control | 156 | 17.0 |
| **Treatments (3 µg/ml)** | | |
| Poly-M | 971 | 105.5 |
| Poly-MG | 1074 | 116.7 |
| Heparin | 304 | 33.0 |
| 5 % S-M | 253 | 27.5 |
| 10 % S-M | 244 | 26.5 |
| 2 % S-MG | 258 | 28.0 |
| 5 % S-MG | 269 | 29.2 |

## E. Coagulation Time Measurements

The recorded plasma coagulation times for the sulfated alginate samples are listed in Table E 1, including the coagulation times for unmodified poly-M and poly-MG alginates, measured at the two highest concentrations in the selected dose range. Times were recorded from added RECALMIX, as described in the HEPTEST® protocol, to visible solidification of the plasma.

**Table E 1: Recorded coagulation times (s) of normal human plasma supplemented with factor Xa and treated with poly-M and poly-MG alginates either unmodified or sulfated using chlorosulfonic acid concentrations of 2 %, 5 % and 10 %.**

| | Coagulation time (s) | | | | | |
|---|---|---|---|---|---|---|
| **Concentration (µg/ml)** | **Poly-M** | **Poly-MG** | **5 % S-M** | **10 % S-M** | **2 % S-MG** | **5 % S-MG** |
| **0** | | | 21 | 21 | 21 | 21 |
| **7.0** | | | 27 | 24 | 22 | 24 |
| **13.9** | | | 29 | 26 | 25 | 30 |
| **27.8** | | | 34 | 34 | 29 | 42 |
| **55.6** | 21 | 23 | 43 | 52 | 35 | 78 |
| **111.2** | 20 | 24 | 72 | 81 | 37 | 227 |

The plasma coagulation times of the heparin-treated samples are listed in Table E 2.

**Table E 2: Recorded coagulation times (s) of normal human plasma supplemented with factor Xa and treated with increasing concentrations of heparin.**

| | Coagulation time (s) |
|---|---|
| **Concentration (µg/ml)** | **Heparin** |
| **0** | 21 |
| **1.7** | 32 |
| **3.4** | 56 |
| **7.0** | 132 |
| **13.9** | 513 |